

Regional volcanism of northern Zealandia: post-Gondwana break-up magmatism on an extended, submerged continent

Mortimer N. ^{1,*}, Gans P. B. ², Meffre S. ³, Martin C. E. ⁴, Seton M. ⁵, Williams S. ⁵, Turnbull R. E. ¹, Quilty P. G. ³, Micklethwaite S. ⁶, Timm C. ⁷, Sutherland R. ⁸, Bache Francois ⁹, Collot Julien ¹⁰, Maurizot P. ¹⁰, Rouillard P. ¹⁰, Rollet N. ¹¹

¹ GNS Science, Dunedin, New Zealand

² Department of Earth Science, University of California, Santa Barbara, USA

³ Department of Earth Sciences, University of Tasmania, Hobart, Australia

⁴ Department of Geology, University of Otago, Dunedin, New Zealand

⁵ School of Geosciences, University of Sydney, Australia

⁶ School of Earth, Atmosphere and Environment, Monash University, Melbourne, Australia

⁷ GNS Science, Lower Hutt, New Zealand

⁸ School of Geography, Environment and Earth Sciences, Victoria University of Wellington, New Zealand

⁹ Santos Ltd., Adelaide, Australia

¹⁰ Service Géologique de Nouvelle Calédonie, Nouméa, New Caledonia

¹¹ Geoscience Australia, Canberra, Australia

* Corresponding author : N. Mortimer, email address : n.mortimer@gns.cri.nz

Abstract :

Volcanism of Late Cretaceous–Miocene age is more widespread across the Zealandia continent than previously recognized. New age and geochemical information from widely spaced northern Zealandia seafloor samples can be related to three volcanotectonic regimes: (1) age-progressive, hotspot-style, low-K, alkali-basalt-dominated volcanism in the Lord Howe Seamount Chain. The northern end of the chain (c. 28 Ma) is spatially and temporally linked to the 40–28 Ma South Rennell Trough spreading centre. (2) Subalkaline, intermediate to silicic, medium-K to shoshonitic lavas of >78–42 Ma age within and near to the New Caledonia Basin. These lavas indicate that the basin and the adjacent Fairway Ridge are underlain by continental rather than oceanic crust, and are a record of Late Cretaceous–Eocene intracontinental rifting or, in some cases, speculatively subduction. (3) Spatially scattered, non-hotspot, alkali basalts of 30–18 Ma age from Loyalty Ridge, Lord Howe Rise, Aotea Basin and Reinga Basin. These lavas are part of a more extensive suite of Zealandia-wide, 97–0 Ma intraplate volcanics. Ages of northern Zealandia alkali basalts confirm that a late Cenozoic pulse of intraplate volcanism erupted across both northern and southern Zealandia. Collectively, the three groups of volcanic rocks emphasize the important role of magmatism in the geology of northern Zealandia, both during and after Gondwana break-up. There is no compelling evidence in our dataset for Late Cretaceous–Paleocene subduction beneath northern Zealandia.

43 **Introduction**

44
45 Zealandia is a 4.9 Mkm² continent that was formerly a part of Gondwana and now lies 94%
46 submerged in the SW Pacific Ocean (Luyendyk 1995; Mortimer *et al.* 2017) (Fig. 1). It consists
47 of a basement of Cambrian to Early Cretaceous terranes and batholiths (Austral Superprovince)
48 and a cover of Late Cretaceous to Holocene sedimentary basins (Zealandia Megasequence;
49 Mortimer *et al.* 2014a). A major tectonic feature of Zealandia is the modern day Pacific-
50 Australia plate boundary (Alpine Fault-Hikurangi Trench in Fig. 1). This divides Zealandia into
51 northern and southern parts and is responsible for Miocene to Holocene subduction-related
52 volcanic rocks on the North Island of New Zealand. In addition to Neogene subduction-related
53 volcanism, Zealandia has a record of different styles and compositions of protracted, scattered,
54 low-volume volcanism that is not related to subduction (Cole 1986; Weaver & Smith 1989;
55 Panter *et al.* 2006; Tulloch *et al.* 2009; Timm *et al.* 2010). This intraplate volcanism erupted in
56 New Zealand sedimentary basins from the Late Cretaceous to the Holocene (Mortimer *et al.*
57 2014a). Zealandia intraplate volcanic rocks share a broadly similar age range and composition
58 with those in formerly adjacent West Antarctica and Australia (Johnson *et al.* 1989). These now-
59 dispersed lavas have previously been described as a Diffuse Alkaline Magmatic Province
60 (DAMP; Finn *et al.* 2005).

61 The datasets used to characterise and explain Zealandia intraplate magmatism have, to
62 date, mostly come either from onland New Zealand or from islands and dredges in southern
63 Zealandia which lies on the present day Pacific Plate (e.g. Cole 1986; Gamble *et al.* 1986; Herzer
64 *et al.* 1989; Weaver & Smith 1989; Baker *et al.* 1994; Tappenden 2003; Nicholson & Black
65 2004; Cook *et al.* 2004; Hoernle *et al.* 2006; Panter *et al.* 2006; Sprung *et al.* 2007; Coombs *et*
66 *al.* 2008; Tulloch *et al.* 2009; Timm *et al.* 2009, 2010; McCoy-West *et al.* 2010; van der Meer *et*
67 *al.* 2013; Scott *et al.* 2015). In contrast, examples of intraplate magmatism from offshore

68 northern Zealandia, on the present day Australian Plate are far fewer (e.g. Green 1973; Baubron
69 *et al.* 1976; McDougall *et al.* 1981; Mortimer *et al.* 1998; Timm *et al.* 2010; Dadd *et al.* 2011;
70 Higgins *et al.* 2011; Nicholson *et al.* 2011). In large part this is because New Zealand and its
71 subantarctic islands have the most accessible igneous rock occurrences. Most published accounts
72 of intraplate volcanism in both northern and southern Zealandia preceded the use of the name
73 Zealandia as a continent, and were equivocal as to the geological setting of the Lord Howe Rise
74 and Norfolk Ridge. As such the older literature on the intraplate magmatism of the Zealandia
75 continent lacks context and is not comprehensive.

76 In this paper we present 18 Ar-Ar ages, two U-Pb ages, six micropaleontological ages, 22
77 whole rock geochemical analyses and 19 Nd isotope analyses from Late Cretaceous to Miocene
78 volcanic rock samples on the Loyalty, Fairway and Norfolk ridges, Lord Howe Rise, and in the
79 New Caledonia, Aotea and Reinga basins (Fig. 1). These samples were collected in rock dredges
80 on the GEORSTOM, AUSFAIR, IPOD, DRASP and ECOSAT cruises (Table 1; Monzier &
81 Vallot 1983; Colwell *et al.* 2006; Collot *et al.* 2013; Bache *et al.* 2014a; Seton *et al.* 2016a,
82 respectively).

83 Our new dataset adds considerably to the existing meagre collection of igneous rocks from
84 northern Zealandia. In turn this enables a more complete picture of the magmatism across all of
85 Zealandia to be presented and explained. This paper builds on and extends syntheses of intraplate
86 volcanism by Finn *et al.* (2005), Hoernle *et al.* (2006), Timm *et al.* (2010) and Bryan *et al.*
87 (2012), and the Zealandia stratigraphic-magmatic framework of Mortimer *et al.* (2014a). It is a
88 companion paper to the dating of Lord Howe Rise lavas by Higgins *et al.* (2011), Reinga Basin
89 sedimentary rock interpretations of Browne *et al.* (2016) and investigations of the South Rennell
90 Trough spreading centre by Seton *et al.* (2016b).

91

92

93 **Northern Zealandia Framework**

94

95 The three main emergent areas of northern Zealandia are New Zealand's North Island, the west
96 coast of New Zealand's South Island and New Caledonia (Fig. 1). Continental basement of
97 Paleozoic-Mesozoic accreted terranes is exposed in all three places. Several small islands, island
98 groups, reefs and atolls pockmark northern Zealandia. The largest of these are the Three Kings,
99 Norfolk, Lord Howe, Chesterfield and Loyalty islands. The submerged part of northern
100 Zealandia is dominated by the 2000 x 300 km Lord Howe Rise. East and west of this lie the
101 Dampier and Norfolk ridges and to the southeast are the Challenger Plateau and onland New

102 Zealand. The New Caledonia Trough, a composite Cretaceous and Eocene rift basin (Sutherland
103 *et al.* 2010), is the deepest part of the Zealandia continent and comprises two separate
104 sedimentary basins, New Caledonia and Aotea basins (these, rather than the single trough, are
105 shown in Fig. 1). There has been debate as to whether the basins are floored by continental or
106 oceanic crust (Klingelhoefer *et al.* 2007) and some of the new data reported in this paper bear on
107 this.

108 The exposed bedrock geology of the Three Kings, Norfolk, Lord Howe, Chesterfield and
109 Loyalty islands consists solely of intraplate volcanic rocks. Some islands and seamounts form
110 linear chains and have been proposed as hotspot tracks. The 2600 km long, N-S trending
111 Tasmantids are entirely constructed on oceanic crust except for Cato seamount which impinges
112 on the Zealandia continent (Exon *et al.* 2006). In contrast the 1900 km long, N-S trending Lord
113 Howe Seamount Chain is entirely constructed on Zealandia continental crust except possibly for
114 Horsehead seamount at its northernmost end (Fig. 1). The Tasmantids in the northern Tasman
115 Sea have been shown by McDougall & Duncan (1988) and Quilty (1993) to get younger to the
116 south and these authors presumed a similar younging for the Lord Howe chain. Three other
117 postulated north-south trending hotspot tracks are the 500 km long Capel-Faust-ZONECO5
118 seamounts (van de Beuque *et al.* 1998; Exon *et al.* 2004; Dadd *et al.* 2011), a 900 km linear N-S
119 alignment of seamounts on the eastern Norfolk Ridge (Rigolot 1988) and an 1100 km alignment
120 of seamounts along the western Norfolk Ridge (Fig. 1).

121

122

123 **Methods**

124

125 Methods and analytical laboratories used for whole-rock geochemistry varied depending on
126 sample size. Large (c. >20 g) samples were crushed in a tungsten carbide ring mill and analysed
127 by X-ray fluorescence (XRF) methods at Spectrachem Analytical, Lower Hutt, New Zealand and
128 by fused glass bead ICPMS methods at Washington State University, Pullman, USA (see
129 Mortimer *et al.* 2010 for methods). Small (c. 5-10 g) samples were crushed in agate mortars and
130 analysed by XRF and fused bead ICPMS methods at Washington State University. Two very
131 small (c. <5 g) samples were analysed by laser ICPMS scanning of polished mounts at the
132 University of Tasmania. Except for the latter two samples we report Ba, Cr, Cu, Ni, V, Sc and
133 Zn as analysed by XRF instead of ICPMS.

134 Argon geochronology at the University of California Santa Barbara followed methods
135 described in Mortimer *et al.* (2014b). U-Pb laser ICPMS (inductively coupled plasma mass

136 spectrometry) geochronology at the University of Tasmania followed methods described in Sack
137 *et al.* (2011). Laser ICPMS pyroxene geochemistry methods at the University of Otago, and Nd
138 isotope methods at the University of Otago followed methods described in Mortimer *et al.*
139 (2014b) and Weis *et al.* (2006) respectively.

140 Samples prefixed "P" are archived in GNS Science's National Petrology Reference
141 Collection, as are thin sections, rock powders and mineral separates. Location information,
142 sample descriptions and images, and analytical data are stored in the online Petlab database
143 (<http://pet.gns.cri.nz>; Strong *et al.* 2016).

144

145

146 **Data and results**

147

148 In this section we describe sample petrography, age and composition under three main
149 geological-geographic headings. Sample locations are given in Table 1, a dating summary in
150 Table 2, and full geochemical and Nd isotope data in Tables 3 and 4. Full geochronological,
151 mineral composition and micropaleontological data are given in Supplementary Data Files 1-4.
152 A recurring theme in our dataset is the difficulty in extracting reliable primary geochemical and
153 geochronological signals. The samples still yield useful provisional data, despite small sample
154 size, secondary alteration of mafic minerals and glass to clays, and presence of zeolites,
155 phosphates and carbonate in amygdules, veins and matrix patches. Concentrations of
156 incompatible large-ion-lithophile elements such as Rb, Sr, Th and K are very vulnerable to such
157 secondary alteration and we have avoided using these elements in our interpretations. We have
158 been conservative in our evaluations of the primary composition of the rocks, placing more
159 emphasis on relatively immobile high field strength elements such as Nb, Zr and Ti. We have
160 also increased many statistically geochronological age uncertainties where mineralogy and
161 degassing behaviour indicates poor sample quality.

162 A number of samples display petrographic evidence for low temperature alteration or
163 weathering but we are confident, except where otherwise noted, that most of the ages reported
164 here are primary eruption and crystallization ages, not alteration ages. This is justified by
165 petrographic characteristics of most samples (e.g., pristine igneous zoning and twinning in both
166 phenocrystic and groundmass plagioclase), relatively high radiogenic yields of most samples,
167 and apparent K/Ca ratios from both groundmass and plagioclase separates that are typical of
168 igneous compositions, not hydrothermal phases. Thus we attribute most of the complexities in

169 the argon spectra to the fact that we are dating very low K/Ca materials, and to issues with argon
170 loss and reactor induced recoil from very fine-grained groundmass samples.

171

172

173 *Lord Howe Seamount Chain*

174

175 The Lord Howe seamount chain consists of at least 19 definable volcanic centres (Fig. 1;
176 Missegue & Collot 1987; McDougall & Duncan 1988; Quilty 1993). Prior to this study, lavas
177 had been sampled at Lord Howe Island, Middleton Reef and Gifford Guyot, all in the southern
178 part of the chain (McDougall *et al.* 1981; Mortimer *et al.* 2010; Dadd *et al.* 2011). We present
179 analytical results of samples from the two northernmost seamounts in the chain, the informally
180 named Horsehead seamount (ECOSAT DR15) and from a dredge site c. 50 km north of the
181 Chesterfield Islands (ECOSAT DR16). Both sites yielded only small, altered samples and we
182 acknowledge the data are poor quality and interpretations provisional.

183

184 *Horsehead.* From ECOSAT dredge 15, c. 5 kg of hard cream-coloured shallow water, Mn-
185 crusted limestone was recovered. Several small (0.5-3 cm diameter) pebbles of lava were present
186 between the Mn crust and limestone, with some fully enclosed by the limestone. P82218A and
187 Bi are c. 1.5x1x1cm red-brown plagioclase-pyroxene porphyritic lava pebbles and P82218C a
188 grey lava pebble. No pebbles were fresh, all showed extensive clay alteration.

189 The argon spectrum of groundmass from P82218C was fairly flat (slightly hump-shaped)
190 for the first 75% of gas released with good K/Ca ratios (0.03-0.06) and high radiogenic yields
191 (90-95%) for most of the spectrum (Fig. 2a). Ages and K/Ca ratios both dropped at the highest
192 temperatures due to recoil. We used the broad flat, central step at 27.2 ± 0.5 Ma as a preferred
193 (igneous) age for the sample, expanding the statistical uncertainty to reflect the broad hump
194 shape and likely minor influence of both argon loss and recoil. The argon spectrum of
195 plagioclase from Horsehead P82218Bi started with ages c. 45 Ma and then climbed to c. 75 Ma
196 (see Supplementary Data File 1). K/Ca ratios were 0.013-0.050, reasonable for igneous
197 plagioclases. Radiogenic yields for the low T steps were high. However, there were no good
198 isochrons and we suspect there is excess argon in the higher T steps of this plagioclase. At face
199 value, a preferred age might be c. 48 ± 3 Ma (arbitrary error assigned to bound the ages of the
200 four low T steps) but our confidence in this is low, with an older interpretation possible. We do
201 not use P82218Bi to date Lord Howe Seamount chain volcanism.

202 The hard limestone from Horsehead (DR15A) enclosing some volcanic clasts gave a
203 tentative late Early Miocene age, in agreement with the dated clasts from Horsehead being older.
204 Soft white limestone from Horsehead (DR15C) gave a Pleistocene age (Supplementary Data File
205 2).

206 Because of small sample size, only ICPMS trace elements were able to be obtained from
207 two Horsehead clasts P82218A and 82218C (Table 3). The lack of major element data means
208 they cannot be plotted on Fig. 3a and 3b but petrography and Sc contents indicate a likely
209 basaltic composition (Winchester & Floyd 1977). Zr content and convex-up multi-element
210 normalised patterns with peaks at Ta and Nb match those of typical intraplate basalts (Figs 3c,
211 3d, 4a). Horsehead is arguably the only Lord Howe Seamount Chain volcano to have erupted on
212 oceanic, rather than continental, crust. Yet it has the second lowest initial ϵNd of all four Lord
213 Howe Seamount Chain volcanoes for which we have data (Fig. 5). The initial ϵNd falls within
214 the range of the E-MORBs of the South Rennell Trough immediately to the north and is not
215 dissimilar to a Lord Howe Island lava (Table 4, Fig. 5).

216
217 *Chesterfield Islands.* From ECOSAT dredge 16 c. 0.2 kg of separate, pebble-sized pieces of lava
218 and limestone were obtained. P82221 is a 4x2x1 cm angular piece of subtrachytic, sparsely
219 olivine-phyric basalt. There is fresh plagioclase in the groundmass, but otherwise, groundmass
220 and olivine are completely replaced by clays. P82224 consists of three c. 1 cm pieces of olivine-
221 plagioclase porphyritic altered basalt with a subtrachytic groundmass; clay fills amygdules.

222 The Ar-Ar degassing spectrum of Chesterfield sample P82221 groundmass was similar to
223 Horsehead P82218C. However, P82221 gave not quite as flat a spectrum, and also slightly lower
224 K/Ca ratios and radiogenic yields (see Supplementary Data File 1). We used the flat step in the
225 middle of spectrum to give an interpreted preferred age of 28.1 ± 1.0 Ma (uncertainty boosted to
226 greater than just statistical uncertainty because of the sharper hump). The argon release spectrum
227 of Chesterfield P82224 groundmass was the most difficult to interpret of the three Lord Howe
228 seamount chain groundmass samples. The spectrum was more hump-shaped, with no real flat
229 top, thus there was more evidence for both argon loss and recoil (Supplementary Data File 1).
230 We regard the age of the top of the hump, c. 23 Ma, as a minimum age (Table 2).

231 As with Horsehead, because of the small clast size, only ICPMS trace element data were
232 obtained. Although the multi-element normalised patterns are also convex-up, both analysed
233 Chesterfield samples (P82221 and 82224) have about half the concentration of large ion
234 lithophile elements and high field strength elements than the Horsehead lavas (Fig. 4a), and their

235 Nb/Yb ratio is lower (Fig. 3d). Although the lack of major elements again hinders assignment of
236 a rock name, they have the features of transitional rather than alkaline basalts. Chesterfield lava
237 P82221 has a higher initial ϵ_{Nd} when compared to that of the analysed Horsehead lava (Fig. 5).
238 The reasons for these chemical and isotopic differences are explored in the Discussion section
239 below.

240

241

242 *New Caledonia Basin margins*

243

244 A group of lavas of distinct chemistry and age occur around the margins of the New Caledonia
245 and Fairway Basins in the northern part of northern Zealandia (Figs. 1, 3, 4b, 5). These samples
246 have not been dredged from well-preserved, upstanding volcanic seamounts. Instead they are
247 samples of seismic acoustic basement exposed as relatively subdued, current-swept areas (e.g. Le
248 Noroit, IPOD sites), or on fault scarps that expose rocks older than seismic sedimentary cover
249 (e.g. Nereus Reef, Lansdowne Bank, AUSFAIR sites).

250

251 *Le Noroit Seamounts.* Although described as seamounts, a seismic line (Daniel *et al.* 1977, fig.
252 4) shows that they consist of a broad (c. 100 x 100 km), partly faulted basement high that has not
253 been completely covered by the sediments of the New Caledonia and d'Entrecasteaux basins.
254 ECOSAT dredge 11 was taken from the highest seamount. It yielded no substantial solid
255 basement rock but only manganese crusts (one up to 11 cm thick) and a few dozen c. 2-5 cm
256 diameter manganese nodules. The nodules contained <1 cm angular kernels of pale grey, green
257 and red lava in their cores as well as various calcareous and phosphatic rocks.

258 Automated scanning electron microscopy of 18 polished manganese nodules identified
259 small (7-30 micron), rare (n=15) zircons in two of the lava kernels which were then dated by *in*
260 *situ* LAICPMS methods. For DR11Ei, 10 of the 11 zircons were Paleocene in age and one was
261 Middle Jurassic (Fig. 6). The Paleocene zircons gave an intercept age of 63.8 ± 3.1 Ma that we
262 interpret as the crystallisation age of the lava. The single 168 Ma zircon is probably a xenocryst
263 incorporated in the lava from underlying (continental) crust. The four zircons found in DR11Ev
264 collectively give an intercept age of 65.5 ± 4.2 Ma, within error of DR11Ei.

265 The chemistry of the two Le Noroit lavas reveals them to be trachytes, slightly more
266 siliceous than trachyandesite and showing an iron enrichment trend (Figs. 3a, 3b). Their overall
267 high incompatible element content (Figs 3c, 4b) indicates they are part of an alkaline suite. We

268 explain their relatively low Eu, Nb, Ta and Ti content in part due to fractionation of plagioclase,
269 amphibole, biotite, ilmenite and titanite. The initial ϵNd of Le Noroit lava DR11Fi (Table 4) is
270 slightly more radiogenic than the Lord Howe Seamount Chain lavas (Fig. 5).

271
272 *Lansdowne Bank and Nereus Reef*. Launay *et al.* (1977, fig. 2) and Collot *et al.* (2008, figs 11,
273 13) presented seismic profiles across the northern Fairway Ridge. Two dredges were taken from
274 the northern Fairway Ridge on the ECOSAT cruise, one on the steep, northeast side of the
275 Lansdowne Bank (DR17) and another on the steep, northeast side of Nereus Reef (DR18) (Fig.
276 1). Although 65 km apart, similar lithologies occur in the two dredges and we describe them
277 together.

278 Lansdowne Bank yielded 18 small pieces of hard, dark green-grey, fine to medium grained
279 aphyric lava and volcanoclastic sandstone. About half of these were >10 mm in size (the largest
280 being 15x10x5 mm), and the other half <5 mm. All pieces were angular in shape. The fact that
281 some samples have clean broken faces and very thin (<0.5 mm) crusts on non-broken faces
282 suggested they probably were broken off *in situ* rock outcrops. In thin section the lavas contain
283 many secondary minerals including chlorite and zeolite. From Nereus Reef, a dozen angular
284 pieces of red coloured, hydrothermally altered, veined and brecciated plagioclase-augite
285 porphyritic lava were dredged, the largest was DR18Bi (10x8x6 cm) and the smallest 3-4 cm in
286 size. Despite the obvious alteration of the Lansdowne and Nereus samples, three samples were
287 chosen for Ar-Ar geochronology of groundmass separates and four samples for whole rock
288 geochemistry. Because of the small sample sizes, different samples had to be selected for the
289 different kinds of analysis.

290 All three Ar-Ar dated samples from the northern Fairway Ridge had complex gas release
291 spectra in the form of two humps (e.g. Fig. 2b, see Supplementary Data File 1 for all three
292 spectra). The low temperature humps represent degassing of high K/Ca material, probably clays,
293 and show the combined effects of argon loss and reactor induced recoil. The higher temperature
294 humps had higher K/Ca (0.4-0.8) probably corresponding to degassing of groundmass adularia
295 of hydrothermal origin. The ages in the high-temperature domains climbed to c. 78 Ma in
296 Lansdowne P82230, c. 81 Ma in Lansdowne P82231 and c. 58 Ma in Nereus P82240. Based on
297 the abundance of secondary minerals in thin sections, even the oldest ages in the high-
298 temperature humps are likely to be partly or wholly alteration ages. As such, we interpret these
299 as minimum ages for the stratigraphic ages of the lavas (Table 2) which could actually be as old
300 as Permian or Early Cretaceous.

301 Supporting age information was obtained from Lansdowne Bank limestone DR17Gi. This
302 is a separate sample of hard foraminiferal limestone (not enclosing, or in contact with, any of the
303 lavas); *Miogypsinoides* suggests an earliest Miocene, or possibly latest Oligocene, age and a
304 shallow-water, tropical paleoenvironment. From Nereus Reef, foraminiferal limestone DR18Ci
305 contains c. 30% red clasts similar to the altered volcanics described above. The limestone
306 contains a juvenile *Lepidocyclina* which indicates an Early-Middle Miocene age and a paleo-
307 water depth shallower than c. 100 m.

308 The small sample size and extreme secondary alteration of the northern Fairway Ridge
309 lavas present considerable difficulty in the interpretation of their primary geochemistry. Based
310 on petrography and Sc content, all five samples appear to be altered basaltic andesites and
311 andesites. Zr varies from 39-122 ppm and Ba, Th, Nb, La and Ce show even more inter-sample
312 variation (Table 3, Figs 3c, 4b), but to what extent this variation is primary or secondary is hard
313 to assess. The five northern Fairway ridge lavas overlap in trace element composition with the
314 two Le Noroit lavas, but show more extreme negative depletion in Nb and Ta and, as expected,
315 lower Nb/Yb ratios (Fig. 3d). The initial ϵNd of the Nereus and Lansdowne lavas (Table 4, Fig.
316 5) overlap those of the South Rennell Trough spreading centre, the Lord Howe Seamount Chain
317 and Le Noroit seamounts.

318
319 *AUSFAIR5, Southern Fairway Ridge*. Despite its subdued bathymetric expression south of 26°S,
320 Collot *et al.* (2009) showed that the Fairway Ridge continues as a well-defined magnetic and
321 structural feature that is co-linear with the West Norfolk Ridge and divides the New Caledonia
322 Basin from the Aotea Basin (Fig. 1). Dredge site 5 on the AUSFAIR cruise (Colwell *et al.* 2006)
323 was made on the steep, eastern side of this part of the Fairway Ridge and is labelled as 'Northern
324 West Norfolk Ridge' on the seismic profile of fig. 5 in Exon *et al.* (2007). The dredged rocks
325 included palagonitic volcanic breccias, some carbonate cemented. The largest and freshest
326 volcanic clast was chosen for study, a c. 5x4x2 cm angular plagioclase-augite-hornblende-olivine
327 porphyritic andesite (AUSFAIR-DR5B, P81400). Hornblende is primary and there is no biotite.

328 Hornblende from AUSFAIR5 sample P81400 was Ar-Ar dated. The gas release spectrum
329 yielded a "pseudo-plateau" for c. 90% of gas released (Fig. 2c). We used the step at the top of
330 the central hump, with the highest precision and radiogenic yield, to give an age of 74.1 ± 0.3
331 Ma which we interpret as the age of crystallisation of the lava.

332 Compositionally, the P81400 is a medium-K andesite and has moderate Fe and Zr for its
333 SiO₂ content (Fig. 3a, b, c). On a multi-element normalised diagram (Fig. 4c) the pattern has a

334 prominent negative Nb-Ta anomaly and is similar in shape to the two central Lord Howe Rise
335 trachytes (see below) but is somewhat less fractionated. Analysis of fresh clinopyroxenes from
336 P81400 overlap those of reference basalts from orogenic and non-orogenic settings (Fig. 3e).

337
338 *AUSFAIR3, Central Lord Howe Rise.* Although not spatially on the margins of the New
339 Caledonia Basin, the AUSFAIR3 dredge site is on a fault scarp near the edge of the Fairway
340 Basin (Fig. 1; Colwell *et al.* 2006). Higgins *et al.* (2010) reported U-Pb zircon ages from two
341 lava samples from AUSFAIR-DR3: DR3D1 was described as a trachyte and gave an age of
342 96.9 ± 0.7 Ma and DR3G1 was described as a latite (potassic trachyandesite) and gave an age of
343 74.1 ± 0.7 Ma. In this paper we present the first whole rock geochemical data of these lavas
344 (Table 3). At face value, Fig. 3a indicates they are rhyolites. However, as previously noted by
345 Higgins *et al.* (2010), they lavas contain secondary quartz but no quartz phenocrysts. Because
346 hydrothermal alteration may have increased the silica content of the lavas, we conservatively and
347 loosely refer to both lavas as trachytes. Their high to extreme K₂O content (4.3 and 5.3 wt%)
348 classifies them as shoshonitic and they have the highest large ion lithophile element (Ba, Th)
349 concentrations of our dataset (Fig. 4b). The two AUSFAIR3 lavas are grouped with the New
350 Caledonia Basin margin lavas because they are of Late Cretaceous age, show pronounced
351 negative Nb and Ta anomalies on normalised multielement diagrams (Fig. 4c) and they are not
352 basalts. The AUSFAIR3 lavas show strong compositional similarities with the 97 Ma high-K to
353 shoshonitic rhyolite described from DSDP 207 on the Lord Howe Rise (Fig. 1, Fig. 4e, Tulloch
354 *et al.* 2009).

355
356 *IPOD4, Offshore New Caledonia.* Southwest of New Caledonia, the seafloor descends to the
357 floor of the New Caledonia Basin and is one of the steepest large submarine slopes within
358 Zealandia (with 30° slopes in some places). Just outside the fringing reef near Koumac, near the
359 top of the slope, dredge 4 of the IPOD cruise (IPOD4 in Fig. 1) recovered several dm-sized
360 pieces of glassy, autobrecciated and agglomerated vesicular lava. No volcanic edifice was visible
361 in multibeam bathymetry. Some fractures in the lavas were lined with thin Mn crusts and then
362 further infilled with limestone. Some samples in the dredge consisted of angular lava clasts in a
363 micritic limestone. A thin section of IPOD DR4-VRAC2 (P84022) revealed variably devitrified
364 glass with sparse plagioclase phenocrysts and a thin Mn rind.

365 Two glass and one plagioclase separate from IPOD P84022 were dated by Ar-Ar methods.
366 Degassing spectra from both glass separates were similar, both climbing gradually (one from c.
367 40 up to 45 Ma, the other from c. 45 up to 48 Ma) then plummeting with dropping K/Ca. These

368 spectra (Supplementary Data File 1) showed classic combined recoil and low temperature Ar
369 loss features. In the degassing of plagioclase from the same sample the spectrum was
370 satisfactorily flattish, with most steps within error. The weighted mean plateau age from the first
371 three steps (73% of gas) was 40.0 ± 1.1 Ma. The glass ages had higher apparent precision, but
372 glass in submarine settings has a tendency to trap a non-atmospheric (excess argon) component
373 and thus give spuriously old ages. The plagioclase had very low K/Ca, and tiny signals, but
374 seemed reliable. All things considered, we very provisionally conclude that the ages of all the
375 separates are in rough agreement and that an age of 42 ± 5 Ma should be reported as the age of
376 crystallisation of the lava. Morgans (2014) reported a Late Pliocene age for limestone in cracks
377 in the IPOD4 lava, not inconsistent with an Eocene age of eruption.

378 P84022 is the only glass in our geochemical dataset and, as such, gives reasonably reliable
379 primary compositions (even so, we note it has 4.3 wt% loss on ignition). It is a medium-K dacite
380 that has low Zr, Nb and Ta and the flattest normalised trace element composition (Fig. 4c) of our
381 dataset but only has a small negative Eu anomaly. In this regard it is curiously basalt-like and
382 very different from the other siliceous igneous rocks shown in Fig. 4c and d which, as expected,
383 have higher trace element concentrations. Based on its Nb/Yb ratio (Fig. 3d), P84022 is derived
384 from very depleted mantle.

385
386

387 *Scattered northern Zealandia seamounts*

388

389 The third group of lavas are not part of either the Lord Howe Seamount Chain or acoustic
390 basement. Instead they were sampled from isolated, sometimes partly eroded, volcanic edifices,
391 recognisable as such in multibeam bathymetry or crossing seismic lines. Our new samples are
392 from the Loyalty Ridge, southern Lord Howe Rise, Aotea Basin and Norfolk Ridge area. Similar
393 isolated volcanic centres and cones in northern Zealandia have been described and sampled by
394 van de Beuque *et al.* (1998), Exon *et al.* (2004), Mortimer *et al.* (2010) and Dadd *et al.* (2011),
395 and in southern Zealandia by Timm *et al.* (2010).

396

397 *ECOSAT8, Loyalty Ridge.* ECOSAT dredge 8 was made on an unnamed seamount towards the
398 northwest end of the Loyalty Ridge (Fig. 1). Sample DR08Ai (P82194) was an altered
399 plagioclase porphyritic basalt with c. 30% zeolite and calcite amygdules. The degassing of
400 plagioclase from P82194 gave an excellent flat argon spectrum with a well-defined plateau and
401 isochron (Supplementary Data File 1). K/Ca ratios were reasonably high (0.013), and radiogenic

402 yields were good for most of the spectrum (60-95%). We interpret the 24.6 ± 0.3 Ma weighted
403 mean plateau age of the sample (700-1150°C steps, 98% of gas) as the age of crystallisation of
404 the basalt.

405 The whole rock chemistry of this low-K, high Ti alkali basalt shows the effects of
406 secondary alteration and sediment infiltration. This is particularly noticeable in terms of the high
407 CaO, P₂O₅, LOI and As, and low K₂O. We also note the strong and unusual decoupling/depletion
408 of the rare earth elements (REEs) relative to high field strength elements Nb, Ta, Zr and Hf (Fig.
409 4c) and speculate that this is due to a low REE content in amygdaloidal minerals. Despite this, it
410 is clear from the multi-element normalised pattern in Fig. 4c, that P82194 is of ocean island
411 basalt type affinity and is derived from very enriched mantle (rightmost point in Fig. 3d).

412
413 *GO357, Southern Lord Howe Rise.* A prominent volcanic edifice on the southern Lord Howe
414 Rise was dredged on the GEORSTOM III SUD cruise (GO357 on Fig. 1). A seismic line across
415 the seamount is shown in Bentz (1974, fig. 10) and Launay *et al.* (1977, fig. 2). Geochemical
416 analyses of the dredged calcite amygdaloidal alkali basalt from GO357 (P57144) and of
417 (petrologically unrelated) gabbro basement xenoliths in the basalt (P57145) were presented by
418 Mortimer (2004).

419 For the current study we performed Ar-Ar dating of a plagioclase separate from the
420 xenolith (P57145). This gave a reasonably flat spectrum, though most of the gas came out over a
421 fairly narrow temperature range (Fig. 2d, Supplementary Data File 1). We interpret the weighted
422 mean plateau age of 27.0 ± 0.3 Ma, as the age of rapid cooling of the heated xenolith after
423 eruption and therefore to date, within error, the eruptive age of the enclosing lava.

424 Like the Loyalty Ridge lava, P57144 has high LOI and CaO (Table 3). Except for a small
425 negative Ti anomaly, P57145 has the smooth, convex-up normalised multi-element pattern
426 typical of intraplate ocean island low-K alkali basalts (Fig. 4c). It has the second highest Nb/Yb
427 ratio of our dataset (Fig. 3d) so is derived from very enriched mantle.

428
429 *GO346, Eastern Norfolk Ridge.* A small seamount on the eastern flank of the southern Norfolk
430 Ridge lies approximately 150 km south of Norfolk Island (Fig. 1). It was dredged on the
431 GEORSTOM III SUD cruise (site GO346 on Fig. 1). Subsequently, the Sonne-7 cruise shot a
432 reflection seismic line across the seamount (Hinz 1979). Sample GO346D1 (P78644) is a
433 plagioclase-olivine microporphyrific basalt.

434 Step heating of a groundmass separate from P78644 gave a simple argon release spectrum
435 with an excellent flat plateau for first 58% of gas. The ages decreased at higher temperatures,

436 probably due to recoil effects. Our preferred age for the crystallisation of the basalt is the
437 weighted mean plateau age of 18.1 ± 0.2 Ma (Supplementary Data File 1). P78644 has the lowest
438 Ti and Nb/Y content of the basalts in this seamount group and is a transitional (tholeiitic to
439 mildly alkaline) low-K basalt. This is reflected in its flattish multi-element normalised pattern
440 (Fig. 4c).

441
442 *DRASP19, Reinga Basin.* The Reinga Basin lies c. 70 km east of, and parallel to, the West
443 Norfolk Ridge (Fig. 1). DRASP dredge d19C (DRASP19 on Fig. 1) was made on the
444 northeastern edge of a subdued high on the west side of the basin. The area around the dredge
445 site was not fully surveyed by multibeam bathymetry but, seemingly, the feature is part of a low,
446 shield-like, volcano (Bache *et al.* 2014a, figure on p. 21). Sample d19C (P83198) is a
447 plagioclase-augite-olivine basalt showing extensive clay alteration of olivine and groundmass.

448 Ar-Ar dating of Reinga Basin P83198 groundmass gave results that were difficult to
449 interpret (Supplementary Data File 1). Most gas was released at very low temperatures, probably
450 from clays. K/Ca ratios are adequate (0.13-0.21), but the signals were small. Ages monotonically
451 decreased from 26 Ma indicating a major recoil issue. There was no good plateau or isochron.
452 For a loosely constrained age, we used the first two steps but increased the uncertainty: 25.5 ± 2.5
453 Ma. Foraminifera in two separate limestone samples from the same dredge were dated by
454 Browne *et al.* (2016) as Early Oligocene and Early to Middle Miocene, i.e. close to the lava age.
455 Thin sections show that neither limestone contains volcanoclastic detritus.

456 No ICPMS trace element data are available for P83198 but the high TiO_2 and Nb/Y ratio
457 and the partial but convex-up multi-element normalised diagram (Fig. 4c) show that the lava is a
458 classic sodic alkali basalt.

459
460 *DRASP27, West side of Aotea Basin.* At the foot of slope of the southeastern Lord Howe Rise, a
461 meandering submarine canyon impinges on an ovoid shaped 10 x 5 km low plateau before
462 debouching on the floor of the western Aotea Basin (Bache *et al.* 2014a, figure on p. 23). The
463 plateau has an irregular top but, based on the volcanic rocks recovered, a volcanic-volcanoclastic
464 unit may have been sampled. Sample d27B (P83225; DRASP27 on Fig. 1) is a holocrystalline,
465 coarse-grained basalt comprising interlocking grains of titanite, plagioclase and olivine (the
466 latter altered to clay minerals). In contrast, sample d27C (P83226) is a highly vesicular olivine
467 porphyritic basalt.

468 The overall Ar-Ar gas release spectrum of P83225 groundmass was fairly flat at c. 27 Ma
469 for first 80% of gas released, then dropped to 23 Ma. K/Ca ratios were good (0.3 to 0.6). As a

470 reasonable interpretation, we take the weighted mean pseudoplateau age for the first 80% of gas
471 and increase the uncertainty, giving an age of 27.0 ± 0.5 Ma. For plagioclase from the same
472 sample, the spectrum was fairly flat, but descended slightly from 28.5 to 25.0 Ma. K/Ca ratios
473 are c. 0.025, and radiogenic yield is good at c. 55%. The statistical weighted mean plateau age
474 was 27.7 ± 1.2 Ma. It is reassuring to see agreement in age between the two different materials
475 from the same sample. As a preferred crystallisation age for P83225, we select the plagioclase
476 age of 27.7 ± 1.2 Ma.

477 Groundmass from P83226 degassed in a typical hump-shaped fashion, indicating both low
478 temperature argon loss and recoil. Ages climbed from 26 to 30 Ma, flattened, and then
479 descended to 13 Ma at high temperatures. The central pseudo-plateau part of the spectrum gave
480 an age of 29.4 ± 0.5 Ma. Given that it is not strictly a plateau and we are unsure as to which part
481 of the spectrum is most reliable, we report the age as 29.5 ± 1.5 Ma i.e. overlapping or possibly a
482 little older than P83225. Palynomorphs from mudstone d27H from the same dredge gave an
483 early Teurian (66-60 Ma) age (Browne *et al.* 2016) suggesting a stratigraphic relationship of
484 Paleocene mudstone overlain by Oligocene lava.

485 No ICPMS trace element data are available for Aotea Basin sample P83226 but the Nb/Y
486 ratio and the partial multi-element normalised diagram (Fig. 4c) show that the lava is a mildly
487 alkaline basalt, slightly more enriched than the subalkaline P78644.

488
489 *DRASP2, Aotea Seamount.* This prominent seamount at the southern end of the Aotea Basin has
490 long been speculated to be of volcanic origin (Brodie 1965). It is c. 50x15x0.8 km in size,
491 elongated in an east-northeast direction. DRASP cruise dredge d02 from the western end of the
492 seamount obtained plagioclase-titanaugite-olivine basalts (Bache *et al.* 2014a, figure on p. 14),
493 thus confirming the volcanic origin. In thin section, olivine is completely altered to clay but the
494 groundmass appears fresh and unaltered.

495 The argon dating of groundmass from sample d02C (P83160) gave reliable results. As
496 expected given the very fine-grained matrix, most gas came out at fairly low temperatures. Ages
497 decreased from 22.7 to 22.4 Ma in the first 85% of gas released, then plummeted to ages as low
498 as 7 Ma in the highest T steps (associated with degassing of Ca-rich phases). Such a spectrum is
499 typical of recoil. For most of the spectrum, K/Ca is high (1-3) as is radiogenic signal (85-92%).
500 Given the evidence for recoil, and monotonically descending ages, we interpret the
501 crystallisation age of the lava as 22.5 ± 0.2 Ma.

502 No ICPMS trace element data are available for Aotea Seamount sample P83160 but the
503 Nb/Y ratio >2 , $\text{TiO}_2 >3\text{wt}\%$ and the partial multi-element normalised diagram (Fig. 4c) show
504 that the lava is probably a strongly alkaline to nephelinitic basalt.

505

506

507 **Discussion**

508

509 *Lord Howe Seamount Chain*

510

511 Volcanic rocks have now been sampled and dated from five of the 19 Lord Howe Seamount
512 Chain centres. Limestones dated using foraminifera have been sampled from another two (Figs.
513 1, 7). Our samples from Horsehead and Chesterfield seamounts, although small and poor in
514 quality, are important as they provide data from the northernmost end of the chain. A linear
515 regression through all Lord Howe Seamount chain lava ages gives an average southward rate of
516 younging of c. 60 mm/yr, similar to the subparallel Tasmantids seamount chain (Duncan &
517 McDougall 1988; Quilty 1993) and to alignments of 35-2 Ma volcanic centres in mainland
518 Australia (west of Fig. 1; Knesel *et al.* 2008; Sutherland *et al.* 2012; Davies *et al.* 2015). All
519 chains show a deflection from linearity at c. 26-23 Ma (Figs. 1, 7; Kalnins *et al.* 2015). This
520 indicates, to a first approximation, that the sources of the volcanism of both the Tasmantid and
521 Lord Howe chains were (a) approximately fixed relative to each other, and (b) to some degree
522 coeval. The sparse dating, sometimes only of post-volcanic guyot limestones, does not allow
523 precise bracketing of the age range of volcanism at any one seamount.

524 The volcanism along the Tasmantid and Lord Howe chains marks the northward passage
525 of the Australian Plate over sources of magmatism that are approximately fixed in the mantle.
526 Recent absolute and relative plate motion models (Steinberger *et al.* 2004; Wessel & Kroenke
527 2008; Müller *et al.* 2016) indicate good agreement between predictions from Indo-Atlantic and
528 Pacific hotspots (Fig. 7b). These updated predictions are affirmatively tested with the measured
529 age progression along the Lord Howe chain (Fig. 7b).

530 All Lord Howe Seamount Chain samples lie along the mantle array on a Nb/Yb vs Th/Yb
531 diagram (Fig. 3c). Pearce & Norry (1979) used the Zr/Y ratio of basalts to explore the
532 petrogenesis of alkali and tholeiitic basalts. The Zr/Y ratio of most lavas along the Lord Howe
533 Seamount Chain is between 8 and 14 (Fig. 7a), typical of alkali basalts and their differentiates
534 and of the Tasmantids. The notable exception is Chesterfield which has $\text{Zr/Y} = 3$. The
535 Chesterfield Islands and Bellona platforms represent the largest volume of Lord Howe chain

536 eruptions: they have very shallow water depths (45-80 m), an area of 16,000 km² and resulted
537 from the coalescence of five volcanic centres (Missegue & Collot 1987). The high emplacement
538 rate for the Early Miocene Chesterfield-Bellona eruptive pulse fits with the low Zr/Y which can
539 indicate a high degree of mantle melting. Published geochemical data from the intraoceanic
540 Tasmanid seamount chain (Figs. 4d, 7a) indicate a range of alkaline to subalkaline (including
541 picritic) compositions and therefore also a range of melting regimes with time (Eggins *et al.*
542 1991).

543 Despite all the Lord Howe Seamount Chain volcanoes erupting through continental crust,
544 all lavas have high initial ϵNd and points to a minimal degree of crustal contamination (to low
545 ϵNd) by older basement (Fig. 5). The overall high initial ϵNd and multi-element normalised
546 patterns for the Lord Howe Seamount Chain (with pronounced humps at Nb and Ta) resemble
547 typical low-silica basalts described from the Chatham Islands by Panter *et al.* (2006) and Timm
548 *et al.* (2010). The low silica Chatham Island, and other southern Zealandia locations, lavas also
549 generally have HIMU-type (high $\mu = \text{U/Pb}$) isotopic compositions as opposed to Timm *et al.*'s
550 EM-type (Enriched Mantle) high silica basalts, which have negative slopes descending from Ba
551 (Figs 3d, 4f). Tasmanids isotope data have been interpreted as relating to an EM-I type mantle
552 plume (Eggins *et al.* 1991), seemingly quite different from the Lord Howe Seamount Chain (Fig.
553 5).

554 The space-time relationship of the Lord Howe Seamount Chain to the South Rennell
555 Trough is interesting in the spatial coincidence of hotspot volcanism and backarc spreading. The
556 approximate pole of rotation of c. 45-28 Ma South Rennell Trough spreading is located at the
557 south end of the South Rennell Trough i.e. at Horsehead Seamount (Seton *et al.* 2016b). This age
558 range is bracketed by the 48 ± 3 and 27 Ma lava ages from Horsehead (Fig. 9), and the E-MORBs
559 of the South Rennell spreading centre overlap in geochemical and Nd isotopic composition with
560 Horsehead and Chesterfield lavas (Fig. 5). This match in space, time and composition suggests a
561 genetic relationship between backarc basin spreading and a mantle plume. A plume control on
562 ridge location has been suggested for the western Galapagos by Sinton *et al.* (2003), and Jellinek
563 *et al.* (2003) showed that theoretically, lithospheric separation can capture some or all of a
564 nearby ascending deep mantle plume. The South Rennell Trough and Lord Howe Seamount
565 Chain may be another example of plume-related spreading in a backarc setting (the Eocene-
566 Miocene arc and trench being located to the north and east, possibly under Vanuatu).

567

568

569 *No other age-progressive seamount chains*

570

571 In addition to the Tasmantid and the Lord Howe seamount chain, three other putative north-south
572 trending age-progressive seamount chains have been identified on the eastern Australian Plate
573 (thin, white, dashed lines in Fig. 1). If they showed similar age progressions to the Lord Howe
574 and Tasmantids chains then they would all be expected to become younger to the south at a rate
575 of c. 1.8 Ma per degree of latitude. The existence of the easternmost chain, proposed by Rigolot
576 (1988) linking 3 Ma Norfolk Island with 10 Ma seamounts on the Loyalty Ridge, is not
577 supported by the intervening 23-25 Ma potassic volcanics (Fig. 8c). The 900 km linear chain
578 along the west side of the Norfolk Ridge may yet show a north-south age progression and has
579 been sampled to test this hypothesis (Mortimer *et al.* 2015). The 500 km long Capel-Faust
580 seamount chain may be a relatively short track on the Australian Plate (Dadd *et al.* 2011) but
581 precise age data are still lacking to establish this.

582 With available age data, age-progressive hotspot-style volcanism can only be
583 demonstrated for the Lord Howe and Tasmantid seamount chains (Fig. 8c), restricted to the
584 western part of northern Zealandia. We regard all other widely scattered, Late Cretaceous to
585 Holocene intraplate volcanism in Zealandia (Fig. 8) as derived from asthenospheric and/or
586 lithospheric sources unrelated to postulated deep mantle plumes (Hoernle *et al.* 2006; Timm *et*
587 *al.* 2010).

588

589

590 *Continental crust of Fairway Ridge and New Caledonia Basin*

591

592 The New Caledonia Basin is the longest and most submerged sedimentary basin in Zealandia
593 (Fig. 1). Whereas New Caledonia is underlain by continental crust, no drillhole has yet
594 penetrated basement in the basin or the Fairway Ridge that bounds the basin to the west. Based
595 on geophysical data, a variety of hypotheses of oceanic crust or rifted continental crust have been
596 proposed for the New Caledonia Basin and the Fairway Ridge (see summaries by Lafoy *et al.*
597 2005 and Klingelhoefer *et al.* 2007).

598 Our new dredge data provide the first direct samples of New Caledonia Basin and Fairway
599 Ridge acoustic basement. We regard it as significant that the lavas dredged from Le Noroit
600 seamounts, Lansdowne Bank, Nereus Reef and the AUSFAIR5 site are andesites, basaltic
601 trachyandesites and trachytes. As such, these features cannot be basaltic oceanic crust. The high
602 ϵNd values for the northern Fairway Ridge and Le Noroit lavas (Fig. 4) do not necessarily argue

603 against continental crust basement. Eastern Zealandia Mesozoic greywacke terranes can have
604 high initial ϵNd (Price *et al.* 2015), and lavas that pass through continental crust don't inevitably
605 assimilate it (e.g. Timm *et al.* 2010). The Jurassic zircon in one of Le Noroit lavas does,
606 however, indicate that part of the New Caledonia Basin probably is underlain by continental
607 crust. Middle to Late Jurassic detrital zircons have been found in the Boghen and Central
608 basement terranes of New Caledonia (Adams *et al.* 2009). Our data support a thinned continental
609 crust origin for the New Caledonia Basin and Fairway Ridge (Lafoy *et al.* 2005). In a wider
610 context (Fig. 8a) we regard the c. 88 Ma siliceous volcanics of the Nouméa Basin in New
611 Caledonia (Nicholson *et al.* 2011) as a related syn-rift continental igneous suite, along with the
612 101 Ma Houhora Complex of New Zealand's Three Kings Islands, West Coast South Island
613 granitoids and the Mount Somers Volcanic Group in southern Zealandia (Fig. 1; Tulloch *et al.*
614 2009).

615
616

617 *Late Cretaceous to Eocene subduction?*

618

619 It is important for global plate circuits to establish whether a Late Cretaceous-Paleogene
620 subduction zone existed off or along the eastern edge of northern Zealandia. So far this remains
621 controversial (see review by Matthews *et al.* 2015). The lack of preservation of clear bathymetric
622 volcanic chains and basins means that tectonic models have to be based on geochemical
623 interpretations of dredged lavas. This is fraught with difficulty because mantle melting processes
624 rarely have a direct connection to surficial tectonic regimes, and even compositionally distinctive
625 lavas such as shoshonites, boninites and adakites can form in a variety of melting regimes.
626 Subalkaline basalts and andesites commonly erupt in orogenic (subduction-related) settings.
627 However, non-orogenic basalts and andesites, with broadly similar whole rock compositions to
628 orogenic lavas, are well known, especially from continental rift settings (e.g. Hebrides, Columbia
629 River, Sonora; Morrison 1978, Morris *et al.* 2000, Till *et al.* 2009).

630 Amid the plethora of geochemical discrimination diagrams, negative Nb and Ta anomalies
631 on multi-element normalised plots are considered an indicator of subduction-related process
632 (Baier *et al.* 2008 and references therein). The known partitioning of Ti, Nb and Ta into titanite,
633 FeTi oxides and amphibole could, in principle, lead to depletion of these elements in andesites,
634 dacites and rhyolites through crystal fractionation as magmas move and change between mantle
635 and the surface. However an example of 97 Ma lavas from Mount Somers Volcanic Group in the

636 South Island (Fig. 1) shows that double-normalising to yttrium partially corrects for fractional
637 crystallisation in the basalt, andesite, dacite, rhyolite spectrum. As such, the double-normalised
638 element concentrations of the Mt Somers rhyolite in Fig. 4e are graphically “lowered” to be
639 close to those of the basalt and it is seen that Nb and Ta anomalies do not substantially
640 deepen with increasing SiO₂. There are further complications, however, in that: (a) long-lived
641 earlier subduction (e.g. Cambrian to Early Cretaceous subduction under Gondwana; Mortimer *et al.*
642 2014) may pre-condition the lithospheric mantle such that, when it later melts in an
643 intracontinental setting, the resulting basalts may have negative Nb and Ta anomalies, (b) melts
644 of earlier subduction related basement terranes, plutons or lavas in an intraplate setting may yield
645 siliceous lavas with negative Nb and Ta anomalies, and (c) assimilation of very large amounts of
646 continental crust may, in some cases, impose negative Nb and Ta anomalies on lavas. Thus,
647 relying on negative Nb and Ta anomalies from a few samples to infer paleosubduction may give
648 erroneous and misleading results. This longstanding and important issue cannot be resolved in
649 this paper.

650 So, with all the above caveats, what can be made of the small samples of very altered Late
651 Cretaceous to Eocene intermediate to siliceous volcanic rocks dredged from around the New
652 Caledonia Basin? Taken at face value, the negative Nb and Ta anomalies of the lavas from
653 around the edge of the New Caledonia Basin could be interpreted as having been acquired as a
654 result of Late Cretaceous to Eocene subduction under northern Zealandia (e.g. Schellart *et al.*
655 2006; Nicholson & Black 2004, Nicholson *et al.* 2010). This is supported by the high initial ϵ_{Nd}
656 of the Lansdowne, Nereus and Le Noroit lavas indicating melting of depleted mantle (arguably
657 mantle wedge), and by relatively high Th/Yb at a given Nb/Yb, Pb and large ion lithophile
658 element concentrations (Figs. 3d, 5). Comparing the iron enrichment and SiO₂ vs Zr trends of
659 subduction and intraplate suites from the SW Pacific and selected parts of the world (Fig. 3b, c),
660 we find that, on balance, all continental intraplate igneous suites (even subalkaline ones) tend to
661 have higher FeOT/MgO and Zr than subduction related suites at the same SiO₂ content, even
662 though the best fit lines conceal a huge amount of intra-suite and intra-region variation. The
663 Lansdowne, Nereus, AUSFAIR3, AUSFAIR5 and IPOD lavas mainly plot along low
664 FeOT/MgO and Zr trends (Fig 3b). They also plot well off the mantle array and in the field of
665 continental and oceanic arcs on a Nb/Yb vs Th/Yb diagram (Fig. 3d). However a subduction
666 interpretation for each individual seafloor site is made less certain by various factors: samples
667 from every site are few (1-3 per dredge) and thus show limited compositional range; the lack of
668 primitive basalts adds complications to geochemical interpretation, the two Le Noroit samples

669 are extremely small, the Lansdowne and Nereus lava samples are extremely small and altered.
670 There is also a general absence of independent supporting evidence such as identifiable volcanic
671 chains, accretionary wedges or paleotrenches. The samples lie 250-500 km from the eastern edge
672 of Zealandia so, if they do represent a continental arc, the arc-trench gap is quite wide.

673 An alternative view (and our preferred view) is that the lavas are not subduction-related but
674 are of continental rift (i.e. intraplate) origin. In this scenario they would have acquired their Nb
675 and Ta anomalies via melting of, or interaction with, existing continental crust or from a relict
676 Gondwana slab. The high Zr of the AUSFAIR3 and Le Noroit lavas and high FeOT/MgO of the
677 AUSFAIR5 lava (Figs. 3b, c) suggests they likely to be intracontinental, non-orogenic lavas. The
678 AUSFAIR3 lavas also overlap the field of intraplate A-type granites from Antarctica (Fig. 3d).
679 Taken at face value, the chemistry of the Nereus and Lansdowne would seem to be the most
680 consistent with a subduction-related setting. But these rocks are hydrothermally altered, and
681 yield only minimum Ar-Ar ages. They could be samples of pre-Late Cretaceous (e.g. Darran
682 Suite, Mortimer et al. 2014a) magmatism along the Gondwana margin.

683 The c. 42 Ma dacite dredged by the IPOD cruise from offshore Koumac is especially
684 challenging to interpret. The glass age is speculative and may be affected by either excess argon
685 or argon loss. The trace element (including rare-earth element) concentrations are puzzlingly
686 basalt-like, not dacite-like. The lack of a prominent Eu anomaly suggests little fractionation so
687 possibly the dacite is an anatectic melt of mafic crust (if so, the low Sr/Y indicates a garnet-free
688 source). Taken at face value the low Nb/Yb, Nb, Y+Nb and Zr contents (Figs 3c, 3d, 4c) do
689 indicate a subduction-related origin although some continental rift granites can have the
690 relatively low Y+Nb content of P84022 (Förster *et al.* 1997). The fresh glassy dacite does not
691 have any known onshore correlatives (basalts in the Late Eocene Pandope flysch of the Poya
692 Terrane nappe are metamorphosed). Cluzel *et al.* (2005) reported dates of 27 and 24 Ma from
693 two rare granitoid stocks in onland New Caledonia that also showed multi-element normalised
694 patterns with negative Nb and Ta anomalies.

695

696

697 *Distribution and causes of Zealandia intraplate magmatism*

698

699 *Diffuse Alkaline Magmatic Province.* Finn *et al.* (2005) outlined the extent of a Cenozoic Diffuse
700 Alkaline Magmatic Province (DAMP) in the eastern Australian plate and in Antarctica, now
701 dispersed over an area of c. 40 Mkm². Our new data in the context of a Zealandia continent

702 (Mortimer *et al.* 2017) support the overall concept but, at the same time, require some
703 modification to the DAMP as defined and explained by Finn *et al.* (2005).

704 First, it should be emphasised that widespread intraplate magmatism commenced across
705 Zealandia in the Late Cretaceous (at c. 101 Ma; Tulloch *et al.* 2009) and is not just a Cenozoic
706 phenomenon (Fig. 9). Second, the better definition of continent-ocean boundaries in the SW
707 Pacific region (Mortimer *et al.* 2017), gives a whole new perspective and clarity to the
708 magmatism. DAMP activity is mainly restricted to areas of continental crust, not the intervening
709 oceanic crust. As such, the DAMP is better described as low-volume magmatism mainly
710 scattered across a c. 12 Mkm² area of formerly contiguous Australia, Zealandia and Antarctica
711 continental crust.

712 Both age-progressive and non-age progressive magmatism were lumped into the SW
713 Pacific DAMP by Finn *et al.* (2005). From our analysis we agree that the age, geochemical and
714 isotopic ranges of the Lord Howe and Tasmantid seamount chains fall within those of other
715 Zealandia intraplate magmatism, yet only the seamount chains show an age progression. Finally,
716 although alkaline suites do indeed dominate sampled rocks (the “A” in DAMP), rocks of
717 subalkaline and ultra-alkaline composition are also widespread across Zealandia (Fig. 8; Timm *et al.*
718 2010).

719 The challenge for petrogenetic models is to explain the close juxtaposition in space and
720 time between lavas of very different major element, trace element and isotopic composition.
721 Tulloch *et al.* (2009) observed a general pattern of early Late Cretaceous Zealandia rhyolites and
722 granites being of I-type character, and late Late Cretaceous rhyolites and granites being of more
723 A-type character. They attributed this change to progressively thinning crust allowing mantle-
724 derived magmas to reach the surface. Although it is a generalisation, we see a similar change in
725 Fig. 8 with subalkaline lavas tending to be more abundant in the Cretaceous, and alkaline and
726 ultra-alkaline lavas in the Cenozoic.

727 Finn *et al.* (2005) suggested that long-lived Paleozoic-Mesozoic subduction would likely
728 lead to enrichment of Nb and Ta in the sub-continental lithospheric mantle whereas conventional
729 wisdom indicates that the opposite happens, with these elements being retained in rutile or
730 aluminous clinopyroxene, subducted to greater depths and lost from the sub-continental
731 lithospheric mantle (e.g. Baier *et al.* 2008). Models of Zealandia intraplate magmatism
732 petrogenesis (e.g. Weaver & Smith 1989; Finn *et al.* 2005; Panter *et al.* 2006; Hoernle *et al.*
733 2006; Sprung *et al.* 2007 and Timm *et al.* 2010) are all variations of the edge-driven convection
734 model of King & Anderson (1998). An important observation we can add to this debate is that
735 the features (spatial distribution, age, compositional range) of the non-age progressive igneous

736 rocks are broadly similar in northern and southern Zealandia (Fig. 9). This is despite the two
737 halves of the continent having had very different histories. Since the Late Cretaceous, southern
738 Zealandia has been locked in a passive margin relationship to the Hikurangi Plateau and Pacific
739 Plate. In contrast, the greater bathymetric relief of northern Zealandia suggests more variation in
740 lithospheric thickness. As the crustal and lithospheric structure of Zealandia becomes better
741 known (Mortimer *et al.* 2017), and more volcanoes are sampled and dated, it may be possible
742 more accurately to identify steps in lithospheric thickness and find some spatial control to the
743 intraplate magmatism (cf. Davies *et al.* 2015).

744
745 *Siliceous Large Igneous Province.* As well as the DAMP, another concept that has been
746 introduced to Australasian Mesozoic geology is that of a SLIP (Silicic Large Igneous Province),
747 arising largely from studies of the Cretaceous Whitsunday volcanics in Australia (Bryan 2007;
748 Bryan *et al.* 2012). Bryan (2007, fig. 1) included the Lord Howe Rise in the Whitsunday SLIP,
749 mainly on the basis of rhyolite in DSDP 207 but also on the inferred extent of Cretaceous
750 volcanoclastic rift basins on the Lord Howe Rise. Subsequent seismic and petrological work
751 (Collot *et al.* 2009; Bache *et al.* 2014b; this study) has identified more basins and more silicic
752 igneous rocks in northern Zealandia. While these might seem to support the expansion of a SLIP
753 from mainland Australia onto the Lord Howe Rise, there are a few things to consider: (1) many
754 of the northern Zealandia silicic volcanics ages are younger than the 95 Ma Whitsunday cut-off
755 proposed by Bryan (2007); (2) some of the rocks may possibly be subduction-related, not
756 intraplate (e.g. Nereus, Lansdowne, see above), (3) the rocks may not occur in sufficient volume
757 to define a large igneous province, and (4) Late Cretaceous silicic igneous rocks are not
758 restricted to northern Zealandia but occur in southern Zealandia as well, so is all of Zealandia
759 part of a Late Cretaceous SLIP?

760 In terms of exploring a causal relationship between SLIP magmatism and continental
761 breakup, it should also be noted that, at the latitude of the Whitsunday Islands (currently 26-20°S
762 in coastal Australia), seafloor spreading (Zealandia-Gondwana separation) did not actually start
763 until c. 62 Ma, rather than the oft-quoted c. 85 Ma for Zealandia-Gondwana separation to the
764 south (Gaina *et al.* 1999). Thus the hiatus between the end of SLIP magmatism and spreading is
765 c. 23 m.y. rather than c. 10 m.y.

766
767 *Space-time-composition patterns.* Numerous studies such as those of Cole (1986), Weaver &
768 Smith (1989), Finn *et al.* (2005) and Timm *et al.* (2010), have searched without success for
769 space-time-composition patterns in subsets of Zealandia intraplate lavas - the Horomaka

770 Supersuite of Mortimer *et al.* (2014a). We have compiled all known occurrences of lavas in Fig.
771 8 and show them on schematic palinspastic reconstructions appropriate for their age. Once again,
772 no obvious age trends emerge but some subtle patterns are present e.g. the aforementioned
773 slightly greater abundance of subalkaline lavas in the early Late Cretaceous and ultra-alkaline
774 lavas in the Cenozoic.

775 Although we have not attempted to calculate volumes or fluxes, it is apparent from Figs. 8
776 and 9 that lavas of Late Cretaceous and Oligocene-Neogene age are more common than those of
777 Eocene age. The Late Cretaceous pulse can be understood as magmatism associated with syn-rift
778 deformation prior to, during and immediately after Zealandia breakup from Gondwana. The
779 Oligocene to Neogene pulse of intraplate magmatism is more difficult to explain as it does not
780 coincide with any major plate motion change. To the south of Zealandia, the Emerald Basin
781 opened from c. 45 Ma and this is also when a subduction phase initiated off northern Zealandia
782 (Sutherland *et al.* 2010), propagating south to form a volcanic arc in New Zealand by c. 23 Ma
783 (Cole 1986; Figs. 8b,c). However, the timing as presented is in conflict with the concept of plate
784 motion changes that have been direct driving forces for increased mantle lithosphere melting
785 within Zealandia. It is simply possible that the younger rocks are more easily sampled, by virtue
786 of their higher stratigraphic positions. By the same token, the Late Cretaceous syn-rift
787 magmatism in Zealandia may be far more common, and is therefore underrepresented in Figs. 8a
788 and 9. Magnetic anomalies on the Campbell Plateau and either side of the Aotea Basin
789 (Sutherland 1999, fig. 3) may represent such Late Cretaceous magmatism.

790

791

792 **Conclusions**

793

794 New sampling, dating, and geochemical and isotopic analysis of small and altered volcanic rock
795 samples from the submerged northern Zealandia continent, combined with earlier work, reveal
796 three volcanotectonic regimes (Figs. 8, 9):

797 (1) *age-progressive, Oligocene-Pliocene, alkaline volcanism of the Lord Howe Seamount*
798 *Chain*. Inception of the Lord Howe Seamount Chain as a linear feature began at c. 28 Ma. Prior
799 to that the position of the Lord Howe plume was coincident with the South Rennell Trough, a
800 backarc spreading centre which was active from c. 45-28 Ma. The Lord Howe Seamount Chain
801 is partly coeval with the nearby Tasmantids seamount chain. Although basalts from each chain
802 are derived from melting of different sorts of geochemical and isotopic mantle, positions of both
803 plumes are approximately fixed in the mantle and are well-predicted from plate kinematic

804 modelling. Age-progressive, hotspot-type volcanism is not known from anywhere else in
805 Zealandia.

806 (2) *Late Cretaceous-Paleogene, generally subalkaline intermediate to silicic volcanism*
807 *on and near ridges and rises around the New Caledonia Basin.* Our new samples are of >78 Ma
808 to c. 42 Ma age but similar silicic suites elsewhere in northern Zealandia are as old as 101 Ma.
809 The samples support a continental crust basement for the New Caledonia Basin and Fairway
810 Ridge. The tectonic setting of eruption of most of these lavas, based on geochemistry, is
811 intraplate continental. The very highly-altered Nereus and Lansdowne lavas may have a
812 subduction-related chemistry, but their stratigraphic age is older than their Late Cretaceous
813 hydrothermal overprint. There is no unambiguous volcanic evidence in our dataset for Late
814 Cretaceous to Paleocene subduction beneath northern Zealandia. The c. 42 Ma IPOD4 dacite
815 seems to have the clearest subduction related geochemistry but the correct interpretation of
816 negative Nb and Ta anomalies in ancient lavas is a longstanding problem that we cannot resolve.

817 (3) *alkaline, ultra-alkaline and subalkaline volcanism, scattered across both northern*
818 *and southern Zealandia with no clear spatial or compositional pattern.* Our new northern
819 Zealandia samples are of 30-18 Ma age and reinforce a late Cenozoic pulse in what is otherwise
820 low-volume and long-lived (c. 97 - 0 Ma) intraplate volcanism. Unlike the Lord Howe Seamount
821 Chain lavas, this volcanism is unrelated to any mantle plume. The dispersed magmatism mostly
822 coincides with areas of continental crust within Zealandia, not the surrounding oceanic crust.

823 To date, most of our knowledge of intraplate volcanism on Zealandia has come from the
824 southern part of the continent. The sampling and analysis of offshore northern Zealandia
825 volcanic rocks described in this paper provides a more complete picture of syn-and post-
826 Gondwana breakup magmatism on the entire Zealandia continent.

827

828

829 **Acknowledgements**

830

831 We thank the captains and crews of N/O *Le Noroit*, N/O *Marion Dufresne*, R/V *Southern*
832 *Surveyor*, N/O *l'Alis* and R/V *Tangaroa* without whom the samples described in this paper would
833 not have been obtained. Neville Orr, Ben Durrant, John Simes, Belinda Smith Lyttle, Craig
834 Fraser, Charles Knaack and Diane Johnson provided technical assistance. Information,
835 discussions and/or encouragement from Rick Herzer, Greg Browne, Mark Lawrence, Robert
836 Crookbain, Andy Tulloch and Volkmar Damm are acknowledged. Comments by Ron Hackney,
837 Takehiko Hashimoto and three anonymous reviewers helped improve earlier versions of the

838 manuscript. The analytical work was supported by core funding to GNS Science from the New
839 Zealand Ministry for Business, Employment and Innovation.

840

841

842 REFERENCES

843

844 ADAMS, C. J., CLUZEL, D. & GRIFFIN, W. L. 2009. Detrital-zircon ages and geochemistry of
845 sedimentary rocks in basement Mesozoic terranes and their cover rocks in New Caledonia,
846 and provenances at the Eastern Gondwanaland margin. *Australian Journal of Earth
847 Sciences*, **56**, 1023–1047.

848 BACHE, F., SUTHERLAND, R., MORTIMER, N., BROWNE, G. H., LAWRENCE, M. J. F., BLACK, J.,
849 FLOWERS, M., ROUILLARD, P., PALLENTIN, A., WOELZ, S., WILCOX, S., HINES, B., JURY, S.
850 & ROOP, H. 2014a. Tangaroa TAN1312 voyage report: Dredging Reinga and Aotea basins
851 to constrain seismic Stratigraphy and Petroleum systems (DRASP), NW New Zealand.
852 GNS Science Report 2014/05, 136pp.

853 BACHE, F., MORTIMER, N., SUTHERLAND, R., COLLOT, J., ROUILLARD, P., STAGPOOLE, V. &
854 NICOL, A. 2014b. Seismic stratigraphic record of transition from Mesozoic subduction to
855 continental breakup in the Zealandia sector of eastern Gondwana. *Gondwana Research*, **26**,
856 1060–1078.

857 BAKER, J., GAMBLE, J. A. & GRAHAM, I.J. 1994. The age, geology, and geochemistry of the
858 Tapuaenuku Igneous Complex, Marlborough, New Zealand. *New Zealand Journal of
859 Geology and Geophysics*, **37**, 249–268.

860 BAIER, J., AUDETAT, A. & KEPPLER, H. 2008. The origin of the negative niobium tantalum
861 anomaly in subduction zone magmas. *Earth & Planetary Science Letters*, **267**, 290-300.

862 BAUBRON, J. C., GUILLON, J. H. & RÉCY, J. 1976. Géochronologie par la méthode K/Ar du
863 substrat volcanique de l'île de Maré, archipel des Loyauté (Sud-Ouest Pacifique). *Bulletin
864 BRGM*, **3 série 2**, 165–176.

865 BEIER, C., VANDERKLUYSEN, L., REGELOUS, M., MAHONEY, J. J. & GARBE-SCHÖNBERG, D. 2011.
866 Lithospheric control on geochemical composition along the Louisville Seamount Chain.
867 *Geochemistry, Geophysics, Geosystems*, **12**, Q0AM01, doi:10.1029/2011GC003690.

868 BENTZ, F. P. 1974. Marine geology of the southern Lord Howe Rise, southwest Pacific. In: Burk,
869 C. A.; Drake, C. L. ed. *The geology of continental margins*. New York, Springer-Verlag.
870 Pp. 537–547.

- 871 BRODIE, J. W. 1965. Aotea Seamount, Eastern Tasman Sea. *New Zealand Journal of Geology*
872 *and Geophysics*, **8**, 510–517.
- 873 BROWNE, G. H., LAWRENCE, M. J. F., MORTIMER, N., CLOWES, C. D., MORGANS, H. E. G.,
874 HOLLIS, C. J., BEU, A. G., BLACK, J. A., SUTHERLAND, R. & BACHE, F. 2016. Stratigraphy
875 of Reinga and Aotea basins, NW New Zealand: constraints on regional correlations and
876 reservoir character from dredge samples. *New Zealand Journal of Geology & Geophysics*,
877 **59**, accepted.
- 878 BRYAN, S. E. 2007. Silicic Large Igneous Provinces. *Episodes*, **30**, 20–31.
- 879 BRYAN, S. E., COOK, A., ALLEN, C. M., SIEGEL, C., PURDY, D., GREENTREE, J. & UYSAL, T. 2012.
880 Early-mid Cretaceous tectonic evolution of eastern Gondwana: from silicic LIP
881 magmatism to continental rupture. *Episodes*, **35**, 142–152.
- 882 CLUZEL, D., BOSCH, D., PAQUETTE, J.-L., LEMENNICIER, Y., MONTJOIE, P. & MENOT, R.-P. 2005.
883 Late Oligocene post-obduction granitoids of New Caledonia: a case for reactivated
884 subduction and slab break-off. *Island Arc*, **14**, 254–271.
- 885 COLE, J. W. 1986. Distribution and tectonic setting of late Cenozoic volcanism in New Zealand.
886 *Royal Society of New Zealand Bulletin*, **23**, 7–20.
- 887 COLLOT, J., GELI, L., LAFOY, Y., VIALLY, R., CLUZEL, D., KLINGELHOEFER, F. & NOUZÉ, H. 2008.
888 Tectonic history of northern New Caledonia Basin from deep offshore seismic reflection:
889 relation to late Eocene obduction in New Caledonia, southwest Pacific. *Tectonics*, **27**,
890 TC6006, doi:10.1029/2008TC002263.
- 891 COLLOT, J., HERZER, R. H., LAFOY, Y. & GELI, L. 2009. Mesozoic history of the Fairway-Aotea
892 Basin: implications for the early stages of Gondwana fragmentation, *Geochemistry*,
893 *Geophysics, Geosystems*, **10**, Q12019, doi:10.1029/2009GC002612
- 894 COLLOT, J., ROUILLARD, P., JUAN, C., PATRIAT, M., LENAULT, Y., PRIVAT, A. & MAURIZOT, P.
895 2013. Rapport de mission de la campagne océanographique IPOD (Investigating Post
896 Obduction Deposits) a bord du N/O Alis du 1er au 18 Aout 2012. Rapport Service
897 Géologique de Nouvelle Calédonie 2013(01), 140p. <http://dx.doi.org/10.17600/12100080>
- 898 COLWELL, J., FOUCHER, J.-P., LOGAN, G. & BALUT, Y. 2006. Partie 2, Programme AUSFAIR
899 (Australia–Fairway basin bathymetry and sampling survey) Cruise Report. Les rapports de
900 campagnes a la mer, MD 153/AUSFAIR–ZoNéCo 12 and VT 82/GAB on board R/V
901 Marion Dufresne. Institut Polaire Français Paul Emile Victor, Plouzané, France,
902 OCE/2006/05.

- 903 COOK, C., BRIGGS, R. M., SMITH, I. E. M. & MAAS, R., 2004. Petrology and geochemistry of
904 intraplate basalts in the South Auckland Volcanic Field, New Zealand: evidence for two
905 coeval magma suites from distinct sources. *Journal of Petrology*, **46**, 473–503.
- 906 COOMBS, D. S., ADAMS, C. J., ROSER, B. P. & REAY, A. 2008. Geochronology and geochemistry
907 of the Dunedin Volcanic Group, eastern Otago, New Zealand. *New Zealand Journal of*
908 *Geology and Geophysics*, **51**, 195–218.
- 909 DADD, K. A., LOCMELIS, M., HIGGINS, K. & HASHIMOTO, T. 2011. Cenozoic volcanism of the
910 Capel-Faust Basins, Lord Howe Rise, SW Pacific Ocean. *Deep-Sea Research II*, **58**, 922–
911 932.
- 912 DANIEL, J., JOUANNIC, C., LARUE, B. & RECY, J. 1977. Interpretation of D'Entrecasteaux Zone
913 (north of New Caledonia). International Symposium on Geodynamics in the Southwest
914 Pacific, Nouméa 1976. Editions Technip, Paris, pp. 117–124.
- 915 DAVIES, D. R., RAWLINSON, N., IAFFALDANO, G. & CAMPBELL, I. H. 2015. Lithospheric controls
916 on magma composition along Earth's longest continental hotspot track. *Nature*, **525**, 511–
917 514.
- 918 EGGINS, S. M., GREEN, D. H. & FALLOON, T. H. 1991. The Tasmanid Seamounts: shallow
919 melting and contamination on an EM1 mantle plume. *Earth and Planetary Science Letters*,
920 **107**, 448–462.
- 921 EXON, N. F., QUILTY, P. J., LAFOY, Y. AND AUZENDE, J.-M. 2004. Miocene volcanic seamounts
922 on northern Lord Howe Rise: lithology, age, ferromanganese crusts, and origin. *Australian*
923 *Journal of Earth Sciences*, **51**, 291–300.
- 924 EXON, N. F., HILL, P. J., LAFOY, Y., HEINE, C. & BERNARDEL, G. 2006. Kenn Plateau off
925 northeast Australia: a continental fragment in the southwest Pacific jigsaw. *Australian*
926 *Journal of Earth Sciences*, **53**, 541–564.
- 927 EXON, N. F., LAFOY, Y., HILL, P. J., DICKENS, G. R. & PECHER, I. 2007. Geology and petroleum
928 potential of the Fairway Basin in the Tasman Sea. *Australian Journal of Earth Sciences*,
929 **54**, 629–645.
- 930 FINN, C. A., MULLER, R. D. & PANTER, K. S. 2005. A Cenozoic diffuse alkaline magmatic
931 province (DAMP) in the southwest Pacific without rift or plume origin. *Geochemistry,*
932 *Geophysics, Geosystems*, **6**, Q02005, doi:10.1029/2004GC000723.
- 933 FÖRSTER, H.-J., TISCHENDORF, G. & TRUMBULL, R. B. 1997. An evaluation of the Rb vs. (Y+Nb)
934 discrimination diagram to infer tectonic setting of siliceous igneous rocks. *Lithos*, **40**, 261–
935 293.

- 936 GAINA, C., MULLER, R. D., ROYER, J.-Y. & SYMONDS, P. 1999. Evolution of the Louisiade triple
 937 junction. *Journal of Geophysical Research*, **104**, 12927–12939.
- 938 GAMBLE, J. A., MORRIS, P. A. & ADAMS, C. J. 1986. The geology, petrology and geochemistry of
 939 Cenozoic volcanic rocks from the Campbell Plateau and Chatham Rise. *Royal Society of
 940 New Zealand Bulletin*, **23**, 344–365.
- 941 GREEN, T. H. 1973. Petrology and geochemistry of basalts from Norfolk Island. *Journal of the
 942 Geological Society of Australia*, **20**, 259–272.
- 943 HEAP, A. D., HUGHES, M., ANDERSON, T., NICHOL, S., HASHIMOTO, T., DANIELL, J.,
 944 PRZESLAWSKI, R., PAYNE, D., RADKE, L., AND SHIPBOARD PARTY 2009. Seabed
 945 environments and subsurface geology of the Capel and Faust basins and Gifford Guyot,
 946 Eastern Australia – post survey report. *Geoscience Australia Record*, **2009/22**.
- 947 HERZER, R. H., CHALLIS, G. A., CHRISTIE, R. H. K., SCOTT, G. H. & WATTERS, W.A. 1989. The
 948 Urry Knolls, late Neogene alkaline basalt extrusives, southwestern Chatham Rise. *Journal
 949 of the Royal Society of New Zealand*, **19**, 181–193.
- 950 HIGGINS, K., HASHIMOTO, T., FRASER, G., ROLLET, N. & COLWELL, J. 2011. Ion microprobe
 951 (SHRIMP) U-Pb dating of Upper Cretaceous volcanics from the northern Lord Howe Rise,
 952 Tasman Sea. *Australian Journal of Earth Sciences*, **58**, 195–207.
- 953 HINZ, K. 1979. Report of the *Sonne* southeast Asia cruise 1978: cruise SO-7 – 16.10.1978 –
 954 22.12.1978. *BGR Report*, 6300/79.
- 955 HOERNLE, K., WHITE, J. D. L., VAN DEN BOGAARD P., HAUFF, F., COOMBS, D. S., WERNER, R.,
 956 TIMM, C., GARBE-SCHÖNBERG, D., REAY, A. & COOPER, A. F. 2006. Cenozoic intraplate
 957 volcanism on New Zealand: upwelling induced by lithospheric removal. *Earth and
 958 Planetary Science Letters*, **248**, 350–367.
- 959 JELLINEK, A. M., GONNERMANN, H. M. & RICHARDS, M. A. 2003. Plume capture by divergent
 960 plate motions: implications for the distribution of hotspots, geochemistry of mid-ocean
 961 ridge basalts, and estimates of the heat flux at the core–mantle boundary. *Earth &
 962 Planetary Science Letters*, **205**, 361–378.
- 963 JOHNSON, R. W., KNUTSON, J. & TAYLOR, S. R. 1989. Intraplate volcanism in eastern Australia
 964 and New Zealand. Melbourne, Australian Academy of Sciences.
- 965 KALNINS, L. M., COHEN, B. E., FITTON, J. G., MARK, D. F., RICHARDS, F. D. & BARFOD, D. N.
 966 2015. The East Australian, Tasmantid, and Lord Howe Volcanic Chains: possible
 967 mechanisms behind a trio of hotspot trails. American Geophysical Union, Fall Meeting
 968 2015, abstract #DI41A-2591.

- 969 KING, S. D. & ANDERSON, D. L. 1998. Edge-driven convection. *Earth & Planetary Science*
970 *Letters*, **160**, 289–296.
- 971 KLINGELHOEFER, F., LAFOY, Y., COLLOT, J., COSQUER, E., GÉLI, L., NOUZÉ, H. & VIALLY, R.
972 2007. Crustal structure of the basin and ridge system west of New Caledonia (southwest
973 Pacific) from wide-angle and reflection seismic data. *Journal of Geophysical Research*,
974 **112**, B11102, doi:10.1029/2007JB005093.
- 975 KNESEL, K. M., COHEN, B. E., VASCONCELOS, P. M. & THIEDE, D. S. 2008. Rapid change in drift
976 of the Australian plate records collision with Ontong Java plateau. *Nature*, 454, 754–757.
- 977 LAFOY, Y., BRODIEN, I., VIALLY, R & EXON, N. F. 2005. Structure of the basin and ridge system
978 west of New Caledonia (Southwest Pacific): a synthesis. *Marine Geophysical Researches*,
979 **26**, 37–50.
- 980 LAUNAY, J., DUPONT, J., LAPOUILLE, A., RAVENNE, C. & DE BROIN, C. E. 1977. Seismic traverses
981 across the northern Lord Howe Rise and comparison with the southern part (south-west
982 Pacific). In: International Symposium on Geodynamics in South-West Pacific, Noumea, 27
983 August–2 September 1976. Paris, Editions Technip. Pp. 155–164.
- 984 LE MAITRE, R.W. 1989. A classification of igneous rocks and glossary of terms. Oxford,
985 Blackwell Scientific Publications.
- 986 LETERRIER, J., MAURY, R. C., THONON, P., GIRARD, D. & MARCHAL, M. 1982. Clinopyroxene
987 composition as a method of identification of the magmatic affinities of paleo-volcanic
988 series. *Earth & Planetary Science Letters*, **59**, 139–2154.
- 989 LUYENDYK, B. P. 1995. Hypothesis for Cretaceous rifting of east Gondwana caused by subducted
990 slab capture. *Geology*, **23**, 373–376.
- 991 MATTHEWS, K. J., WILLIAMS, S. E., WHITTAKER, J. M., MÜLLER, R. D., SETON, M., CLARKE, G. L.
992 2015. Geologic and kinematic constraints on Late Cretaceous to mid Eocene plate
993 boundaries in the southwest Pacific. *Earth-Science Reviews*, **140**, 72–107.
- 994 MCCOY-WEST, A. J., BAKER, J. A., FAURE, K. & WYSOCZANSKI, R. 2010. Petrogenesis and
995 origins of mid-Cretaceous continental intraplate volcanism in Marlborough, New Zealand:
996 implications for the long-lived HIMU magmatic mega-province of the SW Pacific. *Journal*
997 *of Petrology*, **51**, 2003–22045.
- 998 MCDUGALL, I., EMBLETON, B. J. J. & STONE, D. B. 1981. Origin and evolution of Lord Howe
999 Island. *Journal of the Geological Society of Australia*, **28**, 155–176.
- 1000 MCDUGALL, I. & DUNCAN, R. A. 1988. Age progressive volcanism in the Tasmantid
1001 Seamounts. *Earth & Planetary Science Letters* **89**, 207–220.

- 1002 MCMILLAN, N. J., DICKIN, A. P. & HAAG, D. 2000. Evolution of magma source regions in the Rio
1003 Grande rift, southern New Mexico. *Geological Society of America Bulletin*, **112**, 1582–
1004 1593.
- 1005 MISSEGUE, F. & COLLOT, J.-Y. 1987. Etude geophysique du Plateau des Chesterfields (Pacifique
1006 sud-ouest). Resultats preliminaires de la campagne Zoneco de N/O Coriolis. *Comptes*
1007 *Rendu Academie Sciences Paris*, **304 (7), Serie II**, 279–283.
- 1008 MIYASHIRO, A. 1974. Volcanic rock series in island arcs an active continental margins. *American*
1009 *Journal of Science*, **274**, 321–355.
- 1010 MONZIER, M. & VALLOT, J. 1983. Rapport preliminaire concernant les dragages realises lors de
1011 la campagne GEORSTOM III SUD (1975). Office de la Recherche Scientifique et
1012 Technique Outre-Mer (ORSTOM), *Centre de Noumea Geologie- Geophysique Rapport*, **2-**
1013 **83**. 77 p.
- 1014 MORGANS, H. E. G. 2014. Foraminiferal biostratigraphy from New Caledonia IPOD dredge
1015 samples. *GNS Science Consultancy Report*, **2014/223**.
- 1016 MORRIS, G. A., LARTSON, P. B. & HOOPER, P. R. 2000. 'Subduction style' magmatism in a non-
1017 subduction setting: the Colville Igneous Complex, NE Washington state, USA. *Journal of*
1018 *Petrology*, **41**, 43–67.
- 1019 MORRISON, M. A. 1978. The use of "immobile" trace elements to distinguish the palaeotectonic
1020 affinities of metabasalts: applications to the Paleocene basalts of Null and Skye, northwest
1021 Scotland. *Earth & Planetary Science Letters*, **39**, 407–416.
- 1022 MORTIMER, N. 2004. Basement gabbro from the Lord Howe Rise. *New Zealand Journal of*
1023 *Geology and Geophysics*, **47**, 501–507.
- 1024 MORTIMER, N., HERZER, R. H., GANS, P. B., PARKINSON, D.L. & SEWARD, D. 1998. Basement
1025 geology from Three Kings Ridge to West Norfolk Ridge, southwest Pacific Ocean:
1026 evidence from petrology, geochemistry and isotopic dating of dredge samples. *Marine*
1027 *Geology*, **148**, 135–162.
- 1028 MORTIMER, N., HERZER, R. H., GANS, P. B., LAPORTE-MAGONI, C., CALVERT, A. & BOSCH, D.
1029 2007. Oligocene–Miocene tectonic evolution of the South Fiji Basin and Northland
1030 Plateau, SW Pacific Ocean: Evidence from petrology and dating of dredged rocks. *Marine*
1031 *Geology*, **237**, 1–24.
- 1032 MORTIMER, N., HAUFF, F. & CALVERT, A. C. 2008a. Continuation of the New England Orogen,
1033 Australia, beneath the Queensland Plateau and Lord Howe Rise. *Australian Journal of*
1034 *Earth Sciences*, **55**, 195–209.

- 1035 MORTIMER, N., DUNLAP, W. J., PALIN, J. M., HERZER, R. H., HAUFF, F. & CLARK, M. 2008b.
1036 Ultra-fast early Miocene exhumation of Cavalli Seamount, Northland Plateau, Southwest
1037 Pacific Ocean. *New Zealand Journal of Geology and Geophysics*, **51**, 29–42.
- 1038 MORTIMER, N., GANS, P. B., PALIN, J. M., MEFFRE, S., HERZER, R. H. & SKINNER, D. N. B. 2010.
1039 Location and migration of Miocene–Quaternary volcanic arcs in the SW Pacific region.
1040 *Journal of Volcanology and Geothermal Research*, **190**, 1–10.
- 1041 MORTIMER, N., GANS, P. B., HAUFF, F. & BARKER, D. H. N. 2012. Paleocene MORB and OIB
1042 from the Resolution Ridge, Tasman Sea. *Australian Journal of Earth Sciences*, **59**, 953–
1043 964.
- 1044 MORTIMER, N., RATTENBURY, M. S., KING, P. R., BLAND, K. J., BARRELL, D. J. A., BACHE, F.,
1045 BEGG, J. G., CAMPBELL, H. J., COX, S. C., CRAMPTON, J. S., EDBROOKE, S. W., FORSYTH, P.
1046 J., JOHNSTON, M. R., JONGENS, R., LEE, J., LEONARD, G. S., RAINE, J. I., SKINNER, D. N. B.,
1047 TIMM, C., TOWNSEND, D. B., TULLOCH, A. J., TURNBULL, I. M. & TURNBULL, R.E. 2014a.
1048 High-level stratigraphic scheme for New Zealand rocks. *New Zealand Journal of Geology
1049 and Geophysics*, **57**, 402–419.
- 1050 MORTIMER, N., GANS, P. B., PALIN, J. M., HERZER, R. H., PELLETIER, B. & MONZIER, M. 2014b.
1051 Eocene and Oligocene basins and ridges of the Coral Sea–New Caledonia region: Tectonic
1052 link between Melanesia, Fiji, and Zealandia. *Tectonics*, **33**, doi:10.1002/2014TC003598.
- 1053 MORTIMER, N., PATRIAT, M., AGRANIER, A., BASSOULLET, C., CAMPBELL, H., DURANCE, P.,
1054 AMANN, M., ETIENNE, S., GUÉRIN, C., JORDAN, N., JUAN, C., MENGIN, M., PITEL, M.,
1055 ROUSSEL, C. & SOETAERT, F. 2015. The VESPA research cruise (Volcanic Evolution of
1056 South Pacific Arcs): a voyage of discovery to the Norfolk, Loyalty and Three Kings
1057 Ridges, northeast Zealandia. *Geoscience Society of New Zealand Miscellaneous
1058 Publication*, **143A**, 98–99.
- 1059 MORTIMER, N., CAMPBELL, H. J., TULLOCH, A. J., KING, P. R., STAGPOOLE, V. M., WOOD, R. A.,
1060 RATTENBURY, M. S., SUTHERLAND, R., ADAMS, C. J., COLLOT, J. & SETON, M. 2017.
1061 Zealandia: Earth's hidden continent. *GSA Today*, **27**, doi: 10.1130/GSAT321A.1.
- 1062 NELSON, C. S., BRIGGS, R. M. & KAMP, P. J. J. 1986. Nature and significance of volcanogenic
1063 deposits at the Eocene/Oligocene boundary, Hole 593, Challenger Plateau, Tasman Sea.
1064 *Initial Reports Deep Sea Drilling Project*, **90**, 1175–1187.
- 1065 NICHOLSON, K. N. & BLACK, P. M. 2004. Cretaceous to early Tertiary basaltic volcanism in the
1066 Far North of New Zealand: geochemical associations and their tectonic significance. *New
1067 Zealand Journal of Geology and Geophysics*, **47**, 437–446.

- 1068 NICHOLSON, K. N., MAURIZOT, P., BLACK, P. M., PICARD, C., SIMONETTI, A., STEWART, A. &
1069 ALEXANDER, A. 2011. Geochemistry and age of the Nouméa Basin lavas, New Caledonia:
1070 evidence for Cretaceous subduction beneath the eastern Gondwana margin. *Lithos*, **125**,
1071 659–674.
- 1072 PANTER, K. S., BLUSZTAJN, J., HART, S.R., KYLE, P.R., ESSER, R. & MCINTOSH, W. C. 2006. The
1073 origin of HIMU in the SW Pacific: evidence from intraplate volcanism in southern New
1074 Zealand and Subantarctic Islands. *Journal of Petrology*, **47**, 1673–1704.
- 1075 PEARCE, J. A. & NORRY, M. J. 1979. Petrogenetic implications of Ti, Zr, Y, and Nb variations in
1076 volcanic rocks. *Contributions to Mineralogy and Petrology*, **69**, 33–47.
- 1077 PEARCE, J. A. & PEATE, D. W. 1995. Tectonic implications of the composition of volcanic arc
1078 magmas. *Annual Review of Earth and Planetary Sciences*, **23**, 251–285.
- 1079 PRICE, R. C., MORTIMER, N., SMITH, I. E. M. & MAAS, R. 2015. Whole-rock geochemical
1080 reference data for Torlesse and Waipapa terranes, North Island, New Zealand. *New
1081 Zealand Journal of Geology and Geophysics*, **58**, 213–228.
- 1082 QUILTY, P. G. 1993. Tasmanid and Lord Howe seamounts: biostratigraphy and
1083 palaeoceanographic significance. *Alcheringa*, **17**, 27–53.
- 1084 RIGOLOT, P. 1988. Prolongement meridional des grandes structures geologiques de Nouvelle-
1085 Caledonie et decouverte de monts sous-marins interpretes comme un jalon dans un nouvel
1086 alignement de hot-spot. *Comptes Rendu Academie Sciences Paris*, **307, Serie II**, 965–972.
- 1087 SACK, P. J., BERRY, R. F., MEFFRE, S., FALLOON, T. J., GEMMELL, J. B. & FRIEDMAN, R. M. 2011.
1088 In situ location and U-Pb dating of small zircon grains in igneous rocks using laser
1089 ablation–inductively coupled plasma–quadrupole mass spectrometry. *Geochemistry,
1090 Geophysics, Geosystems*, **12**, doi 10.1029/2010GC003405
- 1091 SCHELLART, W. P., LISTER, G. S. & TOY, V. G. 2006. A Late Cretaceous and Cenozoic
1092 reconstruction of the Southwest Pacific region: tectonics controlled by subduction and slab
1093 rollback processes. *Earth-Science Reviews*, **76**, 191–233.
- 1094 SCOTT, J. M., TURNBULL, I. M., SAGAR, M. W., TULLOCH, A. J., WAIGHT, T. E. & PALIN, J. M.
1095 2015. Geology and geochronology of the Sub-Antarctic Snares Islands/Tini Heke, New
1096 Zealand. *New Zealand Journal of Geology and Geophysics*, **58**, 202–212.
- 1097 SETON, M., WILLIAMS, S., MORTIMER, N., MEFFRE, S. & MICKLETHWAITE, S. 2016a. Voyage
1098 report for SS2012V06 Eastern Coral Sea Tectonics (ECOSAT), R/V Southern Surveyor,
1099 October–November 2012. *GNS Science Report*, **2016-49**. Lower Hutt, New Zealand: GNS
1100 Science.

- 1101 SETON, M., MORTIMER, N., WILLIAMS, S., QUILTY, P. G., GANS, P. B., MEFFRE, S.,
1102 MICKLETHWAITE, S., ZAHIROVIC, S., MOORE, J. & MATTHEWS, K. J. 2016b. Melanesian
1103 back-arc basin and arc development: constraints from the eastern Coral Sea. *Gondwana*
1104 *Research*, **39**, 77–95.
- 1105 SINTON, J., DETRICK, R., CANALES, J. P., ITO, G. & M. BEHN, M. 2003. Morphology and
1106 segmentation of the western Galápagos Spreading Center, 90.5°–98°W: plume-ridge
1107 interaction at an intermediate spreading ridge. *Geochemistry, Geophysics, Geosystems*, **4**,
1108 8515, doi:10.1029/2003GC000609, 12.
- 1109 SPRUNG, P., SCHUTH, S., MÜNKER, C. & HOKE, L. 2007. Intraplate volcanism in New Zealand:
1110 the role of fossil plume material and variable lithospheric properties. *Contributions to*
1111 *Mineralogy Petrology*, **153**, 669–687.
- 1112 STEINBERGER, B., SUTHERLAND, R. & O'CONNELL, R. J. 2004. Prediction of Emperor-Hawaii
1113 seamount locations from a revised model of global plate motion and mantle flow. *Nature*,
1114 **430**, 167-173.
- 1115 STEINER, A. & STRECK, M. J. 2014. The Strawberry Volcanics: generation of 'orogenic' andesites
1116 from tholeiite within an intra-continental volcanic suite centered on the Columbia River
1117 flood basalt province, USA. *Geological Society, London, Special Publication*, **385**, 281–
1118 302.
- 1119 STOREY, B. C., HOLE, M.J., PANKHURST, R. J., MILLAR, I. L. & VENNUM, W. 1988. Middle
1120 Jurassic within-plate granites in West Antarctica and their bearing on the break-up of
1121 Gondwanaland. *Journal of the Geological Society, London*, **145**, 999–1007.
- 1122 STRONG, D. T., TURNBULL, R. E., HAUBROCK, S. E. & MORTIMER, N. 2016. Petlab: New
1123 Zealand's national rock catalogue and geoanalytical database. *New Zealand Journal of*
1124 *Geology & Geophysics*, **59**, 475–481.
- 1125 SUN, S.-S. & MCDONOUGH, W. F. 1989. Chemical and isotopic systematics of oceanic basalts:
1126 implications for mantle composition and processes. *Geological Society, London, Special*
1127 *Publication*, **42**, 313–345.
- 1128 SUTHERLAND, F. L., GRAHAM, I. T., MEFFRE, S., ZWINGMANN, H. & POGSON, R. E. 2012. Passive-
1129 margin prolonged volcanism, east Australian plate: outbursts, progressions, plate controls
1130 and suggested causes. *Australian Journal of Earth Sciences*, **59**, 983–1005.
- 1131 SUTHERLAND, R. 1999. Basement geology and tectonic development of the greater New Zealand
1132 region: an interpretation from regional magnetic data. *Tectonophysics*, **308**, 341–362.
- 1133 SUTHERLAND, R., COLLOT, J., LAFOY, Y., LOGAN, G. A., HACKNEY, R., STAGPOOLE, V., URUSKI,
1134 C., HASHIMOTO, T., HIGGINS, K., HERZER, R. H., WOOD, R., MORTIMER, N. & ROLLET, N.

1135 2010. Lithosphere delamination with foundering of lower crust and mantle caused
1136 permanent subsidence of New Caledonia Trough and transient uplift of Lord Howe Rise
1137 during Eocene and Oligocene initiation of Tonga–Kermadec subduction, western Pacific.
1138 *Tectonics*, **29**, TC2004, doi:10.1029/2009TC002476.

1139 TAPPENDEN, V. 2003. Magmatic response to the evolving New Zealand Margin of Gondwana
1140 during the Mid-Late Cretaceous. Unpublished Ph.D. thesis, University of Canterbury.

1141 TILL, C. B., GANS, P. B., SPERA, F. J., MACMILLAN, I. & BLAIR, K. D. 2009. Perils of
1142 petrotectonic modeling: a view from southern Sonora, Mexico. *Journal of Volcanology
1143 and Geothermal Research*, **186**, 160–168.

1144 TIMM, C., HOERNLE, K., WERNER, R., HAUFF, F., VAN DEN BOGAARD, P., WHITE, J. D L.,
1145 MORTIMER, N. & GARBE-SCHÖNBERG, D. 2010. Temporal and geochemical evolution of
1146 the Cenozoic intraplate volcanism of Zealandia. *Earth-Science Reviews*, **98**, 38–64.

1147 TULLOCH, A. J., RAMEZANI, J., MORTIMER, N., MORTENSEN, J., VAN DEN BOGAARD, P. & MAAS,
1148 R. 2009, Cretaceous felsic volcanism in New Zealand and Lord Howe Rise (Zealandia) as
1149 a precursor to final Gondwana break-up. *Geological Society, London, Special Publication*,
1150 **321**, 89–118.

1151 VAN DER MEER Q. H. A., SCOTT, J. M., WAIGHT, T. E., SUDO, M., SCHERSTEN, A., COOPER, A. F.
1152 & SPELL, T. L. 2013. Magmatism during Gondwana break-up: new geochronological data
1153 from Westland, New Zealand. *New Zealand Journal of Geology and Geophysics*, **56**, 229-
1154 242.

1155 VAN DE BEUQUE, S., AUZENDE, J.-M., LAFOY, Y. & MISSEGUE, F. 1998. Tectonique et volcanisme
1156 tertiaire sur la ride de Lord Howe (Sud-Ouest Pacifique). *Comptes Rendus de l'Académie
1157 des Sciences, Series IIA*, **326**, 663–669.

1158 WEAVER, S. D. & SMITH, I. E. M. 1989. New Zealand intraplate volcanism. p. 157–188 in
1159 Intraplate volcanism in eastern Australia and New Zealand. Edited by R. W. Johnson, J.
1160 Knutson & S. R. Taylor. Cambridge University Press.

1161 WEAVER, S. D., ADAMS, C. J., PANKHURST, R. J. & GIBSON, I. L. 1992. Granites of Edward VII
1162 Peninsula, Marie Byrd Land: anorogenic magmatism related to Antarctic-New Zealand
1163 rifting. *Transactions of the Royal Society of Edinburgh: Earth Sciences*, **83**, 281–290.

1164 WEIS, D., KIEFFER, B., MAERSCHALK, C., BARLING, J., DE JONG, J., WILLIAMS, G. A., HANANO,
1165 D., PRETORIUS, W., MATTIELLI, N., SCOATES, J. S., GOOLAERTS, A., FRIEDMAN, R. M., AND
1166 MAHONEY, J. B. 2006. High-precision isotopic characterization of USGS reference
1167 materials by TIMS and MC-ICP-MS. *Geochemistry, Geophysics, Geosystems*, **7**, Q08006.

1168 WESSEL, P. & KROENKE, L. W. 2008. Pacific absolute plate motion since 145 Ma: An assessment
1169 of the fixed hot spot hypothesis. *Journal of Geophysical Research, Solid Earth*, 113,
1170 B06101, doi:10.1029/2007JB005499

1171 WINCHESTER, J. A. & FLOYD, P. A. 1977. Geochemical discrimination of different magma series
1172 and their differentiation products using immobile elements. *Chemical Geology*, **20**, 325–
1173 343.

1174
1175

1176 **FIGURE & TABLE CAPTIONS**

1177

1178 **Fig. 1.** Volcanic rock samples of northern Zealandia and the surrounding oceanic crust. Existing
1179 analysed samples from Cole (1986), Nelson *et al.* (1986), McDougall & Duncan (1988), Weaver
1180 & Smith (1989), Quilty (1993), Auzende *et al.* (2000), Stagg *et al.* (2002), Exon *et al.* (2004),
1181 Hoernle *et al.* (2006), Panter *et al.* (2006), Hoffman *et al.* (2008), Collot *et al.* (2009), Heap *et al.*
1182 (2009), Tulloch *et al.* (2009), Timm *et al.* (2010), Mortimer *et al.* (1998, 2007, 2008ab, 2014)
1183 and Scott *et al.* (2015). VMFZ=Vening Meinesz Fracture Zone, CFZ=Cook Fracture Zone.

1184

1185 **Fig. 2.** Ar-Ar degassing spectra of selected samples. Height of rectangles in this figure are $\pm 1\sigma$
1186 but reported ages are $\pm 2\sigma$. Black rectangles are those used to interpret the age. For degassing
1187 spectra, isochron plots, K/Ca plots and raw data for all samples, see Supplementary Data File 1.

1188

1189 **Fig. 3.** Binary geochemistry plots of new analyses. **(a)** Whole rock anhydrous SiO₂ vs.
1190 anhydrous Na₂O+K₂O from Le Maitre (1989). **(b)** Whole rock anhydrous SiO₂ vs FeOT/MgO,
1191 tholeiitic and calcalkaline dividing line from Miyashiro (1974). Lines are second order
1192 polynomial curve fits to various subduction-related and intraplate datasets from McMillan *et al.*
1193 (2000), Nicholson *et al.* (2010), Steiner & Streck (2014) and Petlab (<http://pet.gns.cri.nz>) and
1194 Georoc (<http://georoc.mpch-mainz.gwdg.de/georoc/>) databases. **(c)** Whole rock anhydrous SiO₂
1195 vs Zr. Note that, on the basis of petrography and Sc content, four Lord Howe Seamount Chain
1196 basalts for which there are no SiO₂ analyses are plotted at SiO₂=50 wt% and four northern
1197 Fairway Ridge basaltic andesites are plotted at SiO₂=55 wt%. Lines are second order polynomial
1198 curve fits to various subduction-related and intraplate datasets from same sources as b. **(d)**
1199 Whole rock Nb/Yb vs Th/Yb after Pearce & Peate (1995). Reference Edward VII Peninsula and

1200 Ferrar Antarctic intraplate granites from Storey *et al.* (1988) and Weaver *et al.* (1992). **(e)**
1201 Clinopyroxenes from andesite P81400, reference fields from Leterrier *et al.* (1982).

1202
1203 **Fig. 4.** Multi-element diagrams normalised to primitive mantle of Sun & McDonough (1989).
1204 All analyses have been double normalised to $Y_n=10$ for better comparison between variably
1205 differentiated samples. Cs, Rb, U, K, Pb, Sr and P have been omitted because substantial
1206 secondary alteration effects to their concentrations. **(a)** Lord Howe Seamount Chain lavas (this
1207 study, Mortimer *et al.* 2010, Dadd *et al.* 2011). **(b)** lavas from periphery of New Caledonia Basin
1208 (this study). **(c)** northern Zealandia scattered seamounts (this study). **(d)** seamount chain
1209 reference data from Eggins *et al.* (1991) and Beier *et al.* (2011). **(e)** continental tholeiite
1210 reference data from McMillan *et al.* (2000), Tappenden (2003), Steiner & Streck (2014). **(f)**
1211 Cenozoic southern Zealandia data from Timm *et al.* (2010).

1212
1213 **Fig. 5.** Whole rock Nb/Y vs initial ϵNd of northern Zealandia lavas. Lord Howe Seamount Chain
1214 and New Caledonia Basin margins described in this paper. Back-arc basin basalts (BABBs)
1215 described in Mortimer *et al.* (2014b) and Seton *et al.* (2016b). Degree of alkalinity on x-axis
1216 after Winchester & Floyd (1977), Tasmanid Seamount field from Eggins *et al.* (1991), basement
1217 fields (that span range of initial ϵNd from 100-0 Ma) from Mortimer *et al.* (2008a) and Price *et*
1218 *al.* (2015).

1219
1220 **Fig. 6.** U-Pb Tera-Wasserburg plot of Le Noroit zircons.

1221
1222 **Fig. 7.** **(a)** Co-variation of latitude, age and mean Zr/Y of dated Lord Howe Seamount Chain and
1223 Tasmanid lavas (this study, McDougall *et al.* 1981, Eggins *et al.* 1991, Quilty 1993, Mortimer *et*
1224 *al.* 2010, Dadd *et al.* 2011). **(b)** Predicted Tasmanid and Lord Howe seamount trails based on
1225 the absolute motion of the Australian Plate, anchored at the oldest Lord Howe Island age.
1226 Modelled tracks were computed using two alternative absolute reference frames, one based on
1227 global moving hotspot predictions (Global MHS; Steinberger *et al.* 2004) and the other
1228 computed using a fixed hotspot assumption for the Pacific plate only (Pacific FHS; Wessel &
1229 Kroenke 2008). The plotted Lord Howe Seamount Chain trails neglect any relative motion
1230 across the South Rennell Trough. Because of the way they are derived, the computed lines do not
1231 resolve changes in absolute motion on time scales less than 10 m.y. Triangles show the locations
1232 of actual dated samples.

1233
1234 **Fig. 8.** Age and composition of volcanic rocks of Zealandia summarised on schematic
1235 paleogeographic reconstructions at (a) 60 Ma, (b) 30 Ma and (c) 0 Ma. Lavas erupted in the
1236 preceding 30-40 m.y. are shown in each panel. Data from sources listed in Fig. 1 caption plus
1237 Beier *et al.* (2011), Nicholson *et al.* (2011) and Mortimer *et al.* (2012). Ages rounded to nearest
1238 1 m.y. Some closely-spaced onland occurrences have been combined and/or simplified for
1239 plotting at this generalised map scale. Northern Zealandia is fixed. SFB=South Fiji Basin,
1240 LB=Lau Basin.

1241
1242 **Fig. 9.** Summary of Late Cretaceous-Holocene magmatic chronology of northern and southern
1243 Zealandia. Northern Zealandia has three compositional groups of magmatic rocks, southern
1244 Zealandia just one. Rock compositions are generalised to represent the main types. Data from
1245 sources listed in Fig. 1 caption. TVZ=Taupo Volcanic Zone.

1246
1247 **Table 1.** Location data for samples described in this paper. Marine expedition acronyms, ships
1248 and cruise numbers are as follows: DRASP (Dredging Reinga and Aotea basins to constrain
1249 seismic Stratigraphy and Petroleum systems) R/V *Tangaroa* TAN1312 November 2013;
1250 AUSFAIR (AUStralia-FAIRway basin bathymetry and sampling survey) N/O *Marion Dufresne*
1251 MD153 February 2006; ECOSAT (Eastern COral SeA Tectonics) R/V *Southern Surveyor*
1252 SS2012v06 November 2012; IPOD (Investigation of Post-Obduction Deposits) R/V *l'Alis*
1253 August 2012; GEORSTOM III SUD N/O *Le Noroit* November 1975.

1254
1255 **Table 2.** Reported ages of rocks dated in this study. All quoted numerical age uncertainties in
1256 this table and in the text are $\pm 2\sigma$. High, medium and low quality of Ar-Ar samples is explained
1257 in Mortimer *et al.* (2014b).

1258
1259 **Table 3.** Whole rock geochemical data for this study. Major elements as wt% oxides, trace
1260 elements are ppm. WSU=Washington State University, SCA=Spectrachem Analytical,
1261 UTAS=University of Tasmania, OU=University of Otago. oliv=olivine, cpx=clinopyroxene,
1262 plag=plagioclase, hbl=hornblende, bi=biotite, pptic=porphyritic, zeol=zeolite, cc=calcite.

1263
1264 **Table 4.** Nd isotope data for samples selected from this study (first ten rows), and from
1265 Mortimer *et al.* (2010, 2014b) and Seton *et al.* (2016b) (last nine rows). Chondritic Uniform

1266 Reservoir values used are $^{143}\text{Nd}/^{144}\text{Nd} = 0.512638$ (present day), $^{147}\text{Sm}/^{144}\text{Nd} = 0.1967$, $\lambda^{147}\text{Sm} =$
1267 $6.54 \times 10^{-12}/\text{yr}$.

1268

1269 **Supplementary File 1.** Ar-Ar geochronology data

1270 **Supplementary File 2.** Micropaleontology data

1271 **Supplementary File 3.** LA-ICP-MS U-Pb zircon geochronology data

1272 **Supplementary File 4.** LA-ICP-MS pyroxene compositional data

1273

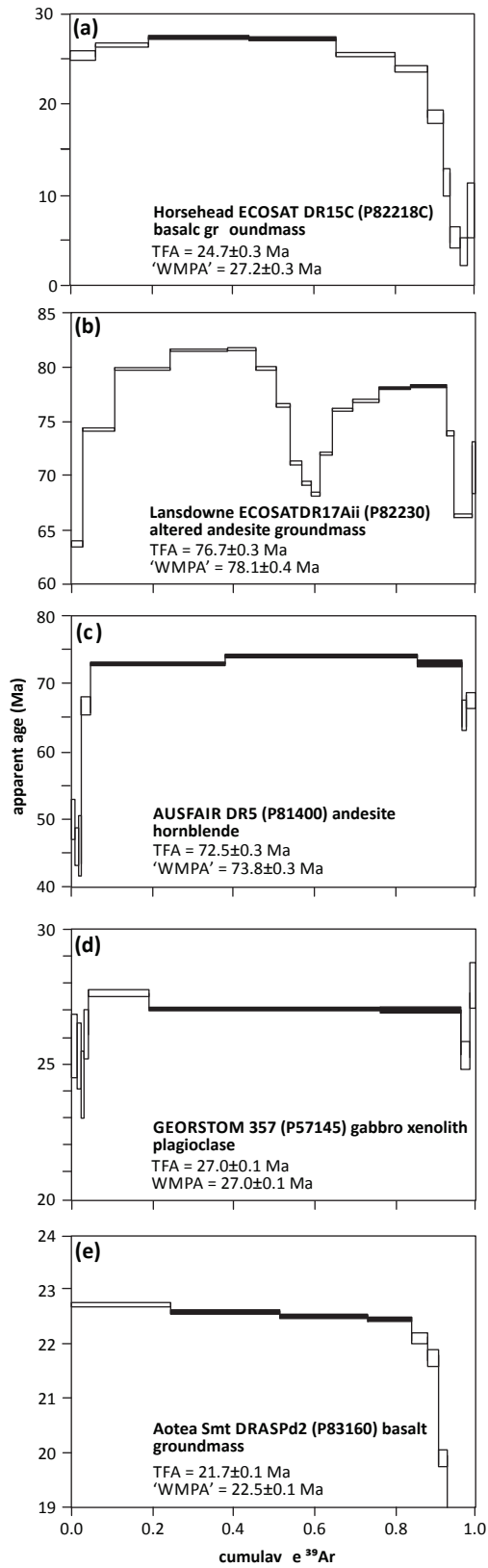
Cruise and dredge	Lat (°S)	Long (°E)	Depth (m)	Site Description	Rocks recovered
Lord Howe Seamount Chain					
ECOSAT DR15	17.6918	158.4713	1850-2600	Horse Head Seamount	Basalts, limestone
ECOSAT DR16	18.7083	158.3688	2500-2800	Chesterfield Plateau, NW side	Basalts, limestone
New Caledonia Basin margins					
ECOSAT DR17	20.1399	160.7699	650-1200	Lansdowne Bank, Fairway Ridge	Altered andesites
ECOSAT DR18	19.9178	160.1923	800-1500	Nereus Reef, Fairway Ridge	Altered andesites
ECOSAT DR11	17.9856	160.7284	2250-2500	Le Noroit Seamounts	Trachyte cores in Mn nodules
AUSFAIR DR03	28.4219	162.7899	1450-1700	Fault scarp, Lord Howe Rise	Rhyolites
AUSFAIR DR05	27.7127	165.2894	c. 2900	Southern Fairway Ridge, east flank	Andesite breccia
IPOD DR4	20.6418	164.1222	c. 710	Offshore from Koumac, New Caledonia	Autobrecciated dacite, limestone
North Zealandia scattered seamounts					
GEORSTOM 357 D1	35.6585	165.9749	770-1250	Seamount, SE Lord Howe Rise	Gabbro xenolith in alkali basalt
GEORSTOM 346 D1	30.4769	168.0898	1840-2300	Seamount, E Norfolk Ridge	Vesicular ol-plag basalt
DRASP d02	37.5588	171.9598	1389-1570	Aotea Seamount	Basanite
DRASP d19	34.5218	169.6479	1715-1777	Seamount, Reinga Basin	Amygdaloidal basalt
DRASP d27B	34.7359	165.6869	1981-2221	Seamount, W side Aotea Basin	Basalts, mudstones
ECOSAT DR08	17.583	164.0078	1300-1500	Seamount, Loyalty Ridge	Amygdaloidal basalt breccia

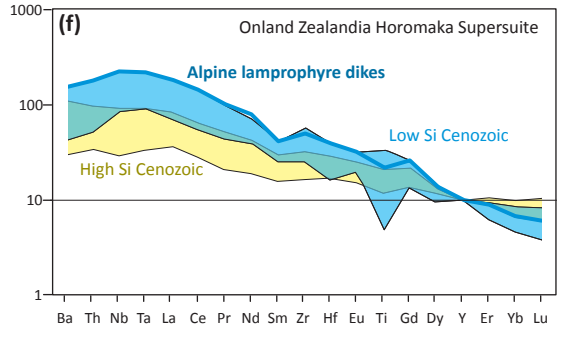
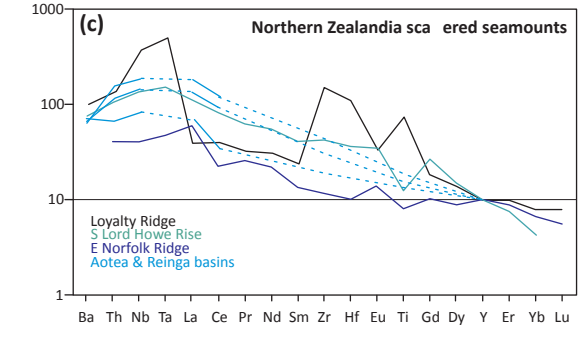
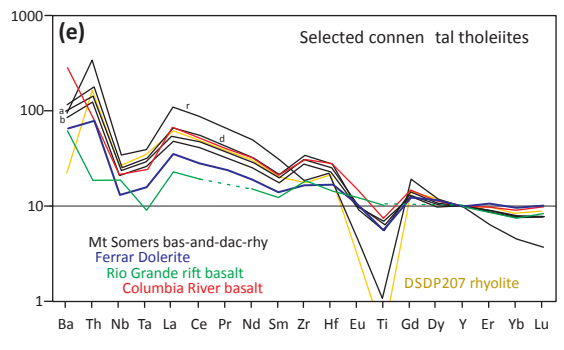
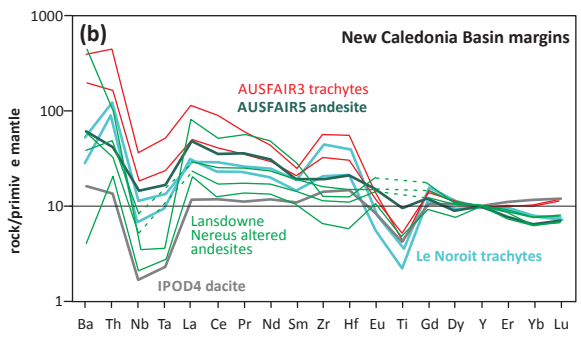
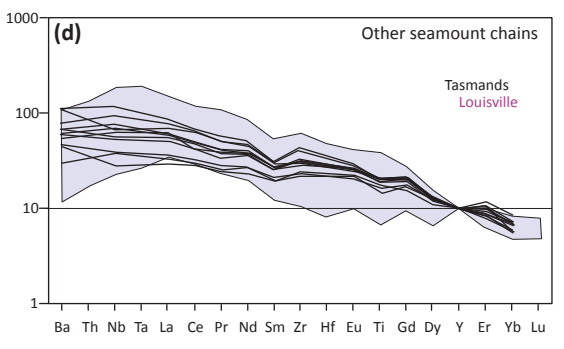
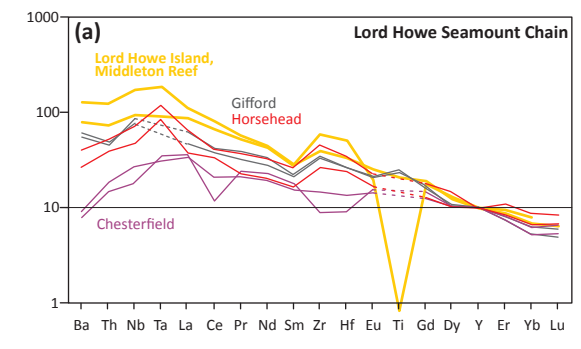
Cruise and dredge #	GNS #	Lab #	Dated material	Quality	Age $\pm 2\sigma$ (Ma)
<i>Lord Howe Seamount Chain</i>					
ECOSAT DR15A Horsehead	na	na	Forams	na	late E Miocene?
ECOSAT DR15B Horsehead	P82218Bi	SB66-25	Ar-Ar plagioclase	Low	48 \pm 3?
ECOSAT DR15B Horsehead	P82218C	SB66-26	Ar-Ar groundmass	Medium	27.2 \pm 0.5
ECOSAT DR15C Horsehead	na	Q1135	Forams	na	Pleistocene
ECOSAT DR16Ai Chesterfield	P82221	SB66-28	Ar-Ar groundmass	Medium	28.1 \pm 1.0
ECOSAT DR16Aiv Chesterfield	P82224	SB66-32	Ar-Ar groundmass	Low	>23
<i>New Caledonia basin margins</i>					
ECOSAT DR11Ei Le Noroit	na	na	U-Pb zircon	na	63.8 \pm 3.1
ECOSAT DR11Ev Le Noroit	na	na	U-Pb zircon	na	65.5 \pm 4.2
ECOSAT DR17A Lansdowne	na	na	Forams	na	E Miocene
ECOSAT DR17Aii Lansdowne	P82230	SB66-3	Ar-Ar groundmass	Low	>78
ECOSAT DR17Aiii Lansdowne	P82231	SB66-4	Ar-Ar groundmass	Low	>81
ECOSAT DR17Gi Lansdowne	na	na	Forams	na	L Olig- E Mio
ECOSAT DR18Bii Nereus	P82240	SB66-5	Ar-Ar groundmass	Low	>58
ECOSAT DR18Ci Nereus	na	na	Forams	na	Early Miocene
AUSFAIR DR05-B1 Fairway Ridge	P81400	SB65-7	Ar-Ar hornblende	High	74.1 \pm 0.3
IPOD DR4-VRAC2 New Caledonia	P84022	SB67-65,66,67	Ar-Ar gmass, plag	Low	42 \pm 5?
<i>North Zealandia scattered seamounts</i>					
ECOSAT DR08Ai Loyalty Ridge	P82194	SB66-44	Ar-Ar plagioclase	High	24.6 \pm 0.3
GEORSTOM 357 D1 Lord Howe Rise	P57145	SB63-5	Ar-Ar plagioclase	High	27.0 \pm 0.3
GEORSTOM 346 D1 Norfolk Ridge	P78644	SB61-108	Ar-Ar groundmass	High	18.1 \pm 0.2
DRASP d19C Reinga Basin	P83198	SB67-62	Ar-Ar groundmass	Low	25.5 \pm 2.5
DRASP d27C Aotea Basin	P83225	SB67-29,60	Ar-Ar gmass, plag	Medium	27.7 \pm 1.2
DRASP d27C Aotea Basin	P83226	SB67-31	Ar-Ar groundmass	Medium	29.5 \pm 1.5

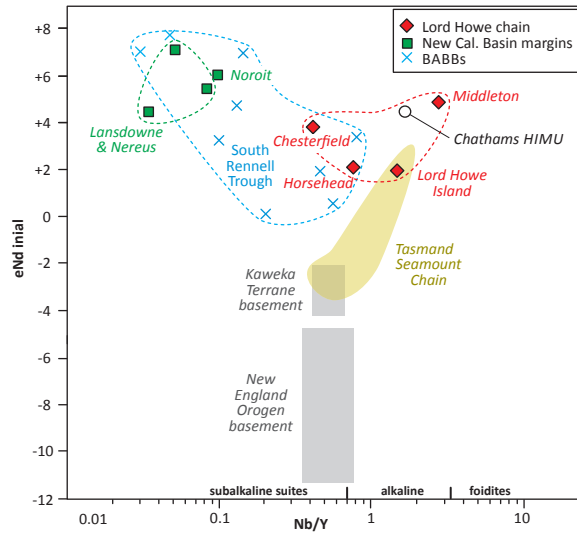
Dredge	GNS#	Approx wt.	Rock Description	Laboratory	SiO2	TiO2	Al2O3	Fe2O3T	MnO	MgO	CaO	Na2O	K2O	P2O5	LOI	Total	As	Ba
Lord Howe Seamount Chain																		
ECOSAT DR15B1 Horsehead	P82218A	10 g	Cpx plag basalt clast in limestone	WSU														122
ECOSAT DR15B1i Horsehead	P82218B	10 g	Cpx plag basalt clast in limestone, dark reddish brown	WSU														149
ECOSAT DR16Ai Chesterfield	P82221	<5 g	Aphyric subtrachytic textured lava, Clay alteration	WSU														52
ECOSAT DR16Aiv Chesterfield	P82224	<5 g	Sparsely plag pttic lava, Dk brown clay alteration	WSU														60
Lord Howe Island LH2	GD6060	250 g	Doleritic plag-cpx basalt, zeol amygdaloidal	SCA, WSU	48.39	2.78	15.23	11.25	0.14	5.67	8.55	3.63	1.47	0.51	2.16	99.78	<1	343
New Caledonia Basin margins																		
ECOSAT DR17Aiv Lansdowne	P82232	<5 g	V strongly altered reddish volc sandstone, basaltic devitrified?	WSU														157
ECOSAT DR17Av Lansdowne	P82233	<5 g	Reddish plag-porphyrific andesite, strongly altered	WSU														183
ECOSAT DR18Bi Nereus	P82239	800 g	Strong hydroth altered (zeol) red aphyric devitrified andesite	WSU	50.35	0.56	17.9	6.83	0.14	5.24	4.01	5.46	1.76	0.46	7.11	99.81	13	15
ECOSAT DR18Bii Nereus	P82240	50 g	Strong hydroth altered red plag-pttic devitrified andesite	WSU														1771
ECOSAT DR18Di Nereus	P82246	20 g	Strong hydroth altered orange red plag-ol basalt	WSU														136
ECOSAT DR11Ei Le Noroit	na	<5 g	Grey aphyric trachyte corestone to Mn nodule	UTAS	58.78	0.77	16.38	6.66	0.03	0.59	4.48	4.7	5.97	1.64		100	36	308
ECOSAT DR11Ev Le Noroit	na	<5 g	Grey aphyric trachyte corestone to Mn nodule	UTAS	58.66	0.96	17.57	6.83	0.03	0.46	3.17	4.58	6.92	0.82		100	8	455
AUSFAIR DR03-G1 Lord Howe Rise	P81397	300 g	Plag-hbl-bi lava, mafics altered	WSU	72.17	0.28	14.13	2.2	0.07	0.58	0.68	2.9	5.29	0.1	1.56	99.96		846
AUSFAIR DR03-G1 Lord Howe Rise	P81397	250 g	Plag-alt'd mafic lava w qtz or zeol amygdules	WSU	67.29	0.78	14.55	5.15	0.07	1.17	0.61	3.29	4.31	0.25	2.46	99.93		913
AUSFAIR DR05-B1 Fairway Ridge	P81400	100 g	Plag cpx hbl oliv andesite clast in volcanic breccia	WSU	50.44	1.2	19.38	7.02	0.05	2.43	6.75	3.81	1.19	1.19	6.1	99.56		244
North Zealandia scattered seamounts																		
GEORSTOM 357 D1 Lord Howe Rise	P57145	50 g	Gabbro xenolith in alkali basalt	SCA, WSU	34.78	1.99	10.04	10.55	0.14	10.47	16.97	2.61	1.41	0.93	9.3	99.19		386.44
GEORSTOM 346 D1 Norfolk Ridge	P78644	200 g	Vesicular ol-plag basalt	OU	47.02	2.44	19.84	10.14	0.16	2.87	9.63	3.53	1.38	0.9	2.15	100.06		
DRASP d02C Aotea Seamount	P83160	500 g	Fresh ol+cpx lava, Minor clay alteration.	SCA	39.87	3.77	11.69	15.39	0.18	8.65	12.2	4.26	1.44	1.27	1.04	99.75	5	432
DRASP d19C Reinga Basin	P83198	500 g	Dark brownish grey olivine micro-phyric basalt, Cc amygdules	SCA	45.06	2.07	13.49	13.8	0.16	8.76	10.32	2.79	0.95	0.63	1.33	99.36	2	281
DRASP d27C Aotea Basin	P83226	2 kg	Sparsely cpx porphyritic, highly vesicular basalt, Clay altered	SCA	42.95	2.11	15.95	12.61	0.26	3.12	11.19	3.75	1.28	2.7	2.96	98.88	51	346
IPOD DR4-VRAC2 New Caledonia	P84022	>100g	Sparsely plag-cpx porphyritic amygdaloidal dacite fresh glass	SCA, OU	65.07	0.49	13.41	5.87	0.16	1.51	3.8	2.98	1.65	0.12	4.33	99.39	3	60
ECOSAT DR08Ai Loyalty Ridge	P82194	>100g	Ol-plag pttic basalt clast in breccia, Cc & zeol amygdules	WSU	53.4	3.27	16.86	7.27	0.08	2.16	9.72	2.35	0.38	1.26	2.92	99.68	51	142

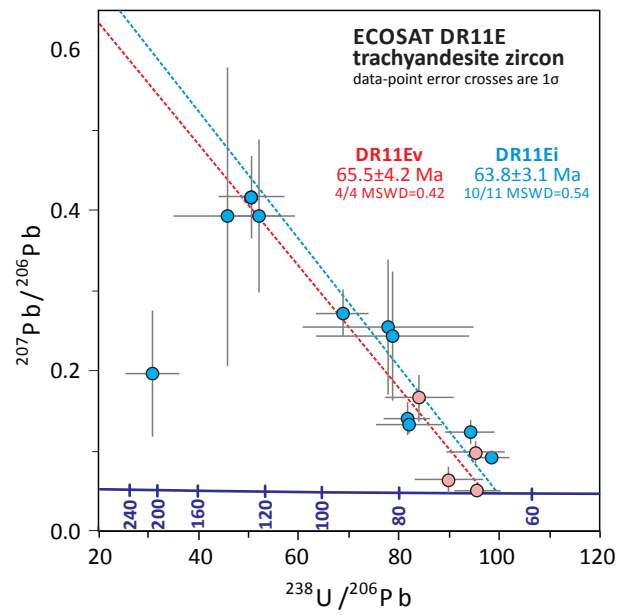
Ce	Cr	Cs	Cu	Dy	Er	Eu	Ga	Gd	Hf	Ho	La	Lu	Nb	Nd	Ni	Pb	Pr	Rb	Sc	Sm	Sr	Ta	Tb	Th	Tm	U	V	Y	Yb	Zn	Zr	GNS#
38.3		0.43		5	2.63	1.86		5.12	4.88	1.01	17	0.33	22.85	18.37		7.04	4.13	10.7	33.3	4.91	431	2.21	0.85	2.23	0.36	1.13		29.86	2.15		195	P82218A
39.12		0.5		5.58	2.76	2.02		6	5.84	1.07	23.95	0.33	27.56	23.46		21.2	5.42	12	32.4	5.96	446	2.58	0.96	2.43	0.37	1.62		24.19	2.25		269	P82218B
29.92		0.89		6.03	3.13	1.94		6.06	3.4	1.21	17.97	0.39	14.82	21.08		1.34	4.7	11.1	33.6	5.41	334	1.02	0.98	1.28	0.43	0.64		36.03	2.47		131	P82221
22.97		0.53		8.13	3.9	2.86		9.37	3.11	1.61	26.99	0.43	13.63	34.02		1.48	7.43	21.6	34.6	8.49	291	1.59	1.4	1.38	0.51	0.59		49.89	2.79		111	P82224
73.4	160	0.08	51	5.66	2.56	2.74	25.2	6.95	6.3	1.03	36.7	0.29	41.1	35.1	72	7	8.83	27.3	19	7.66	690	2.3	1	3.81	0.35	0.9	275	27.4	2.06	102	270	GD6060
11.12		17.48		2.78	1.59	0.88		2.64	1.23	0.6	5.51	0.21	1.36	8.46		5.31	1.76	78.2	23.2	2.35	402	0.99	0.44	1.02	0.22	0.81		16.68	1.38		46	P82232
30.58		5.78		5.5	2.94	1.72		5.65	3.12	1.12	13.18	0.4	3.98	21.77		12.41	4.71	74.8	37.8	5.76	258	2.36	0.91	2.82	0.43	1.02		30.95	2.56		122	P82233
11.48	61	0.23	77	2.95	1.9	0.9	19	2.85	0.97	0.86	7.15	0.27	0.81	9.6	65	4.5	2.01	3.6	14.4	2.51	115	0.06	0.45	1	0.27	0.39	174	23.92	1.59	92	39	P82239
52.49		24.65		4.47	2.34	1.9		5.69	2.18	0.87	31.07	0.28	1.36	36.73		6.87	8.9	207.2	22.8	7.1	512	0.08	0.8	4.8	0.31	1.07		26.37	1.76		80	P82240
19.7		5		4.95	3.18	1.22		5.24	1.73	1.14	20.36	0.41	1.04	19.23		8.67	4.16	69.1	30.2	4.32	114	0.07	0.77	1.79	0.44	1.59		46.76	2.55		72	P82246
63.2	7.5	6.8	248	11.2	6.73	1.5	24.8	11.1	10.4	2.32	34.8	0.88	7.77	43.9	22.1	21.9	10.2	113	10.8	10.7	153	0.63	1.75	13.1	0.94	3.43	136	71.1	6.16	232	374	na
63.1	2.6	5.7	433	10.2	5.71	1.61	27.4	11.2	15.4	2.04	24.6	0.64	10.01	40.5	5.5	36.2	8.91	115	17.6	10.4	134	0.69	1.66	12.7	0.75	2.42	96	54.3	4.68	555	606	na
49.96	6	2.39	18	2.49	1.45	0.75	14	2.65	5.23	0.5	23.07	0.26	7.94	18.45	7	11.05	5.11	122.2	3.4	3.39	181	0.64	0.41	11.39	0.23	1.91	38	13.44	1.55	55	195	P81396
48.66	5	2.53	5	5.63	3.29	1.34	16	5.57	6.29	1.18	23.34	0.53	8.97	26.48	5	12.91	6.49	107.7	12.7	6.02	293	0.65	0.92	9.5	0.52	2.45	45	29.66	3.31	105	239	P81397
35.66	29	0.2	70	3.82	2.12	1.46	18	4.16	3.7	0.78	18.82	0.29	5.92	24.01	34	5.24	5.68	10.9	13.7	4.85	1402	0.39	0.64	2.01	0.31	0.43	167	26.14	1.81	173	122	P81400
106.45	526	0.42	38	8.07	2.64	4.18	18	11.62	8.19	1.28	55.2		73.23	54.69	61	3.7	12.62	31.55	17.23	13.29	917.46	4.56	1.68	6.67	0.3	1.77	136	33.11	1.56	135	346.97	P57145
57.12		0.4		8.92	5.87	3.3		8.47	4.4		56.16	0.57	39.9	41.4		9.86				8.29		2.7		4.8	2.4		63.4	4.55		186.8	P78644	
207	205		71				24				120		128		184	9			40	16		800		13		4	253	42		155	458	P83160
104	345		74				19				57		62		236	6			24	20		579		6		1	174	27		121	208	P83198
43	272		172				19				33		41		114	3			19	28		629		4		5	225	32		153	149	P83226
11.1	<1.0	0.58	4	4.12	2.81	0.75	13	3.31	2.41	0.93	4.25	0.46	0.62	8.57	9	3.69	1.63	14.7	20	2.57	117	0.05	0.61	0.61	0.42	0.36	24	24.5	3.04	81	83.9	P84022
14.72	395	0.1	7	2.06	0.96	1.1	16	2.24	6.94	0.39	5.39	0.12	54.57	8.45	25	0.85	1.8	3.9	29.8	2.14	787	4.22	0.36	2.4	0.13	0.23	209	9.1	0.8	45	350	P82194

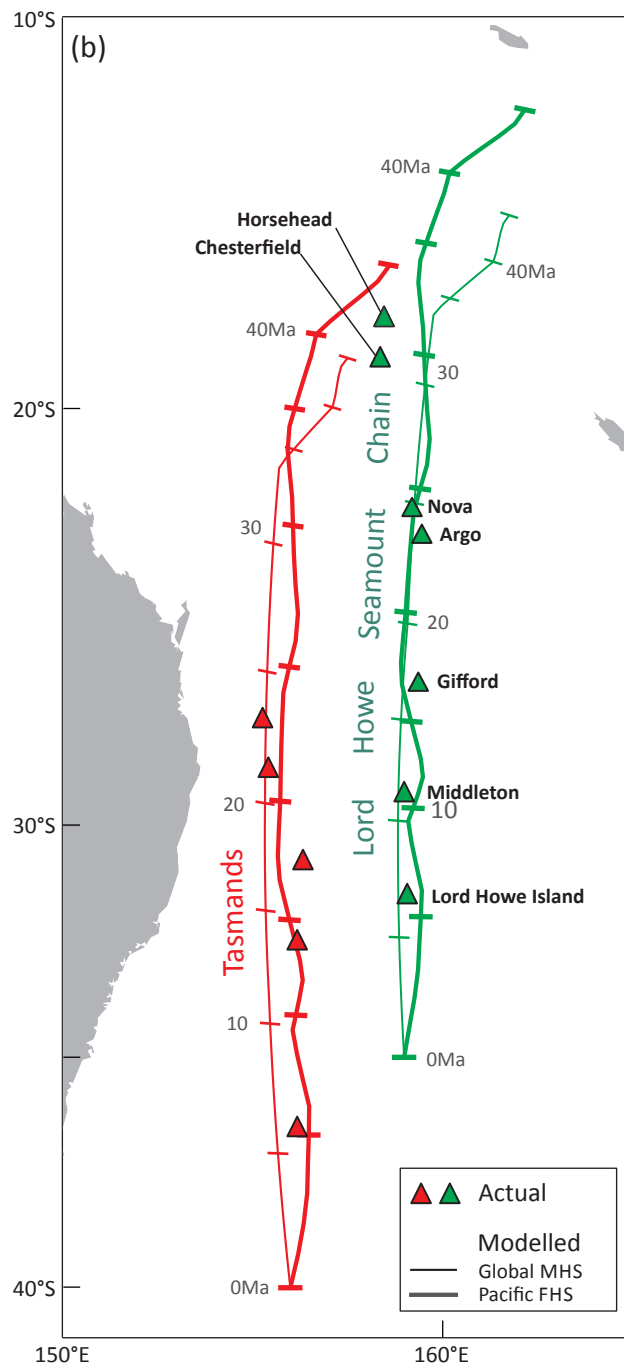
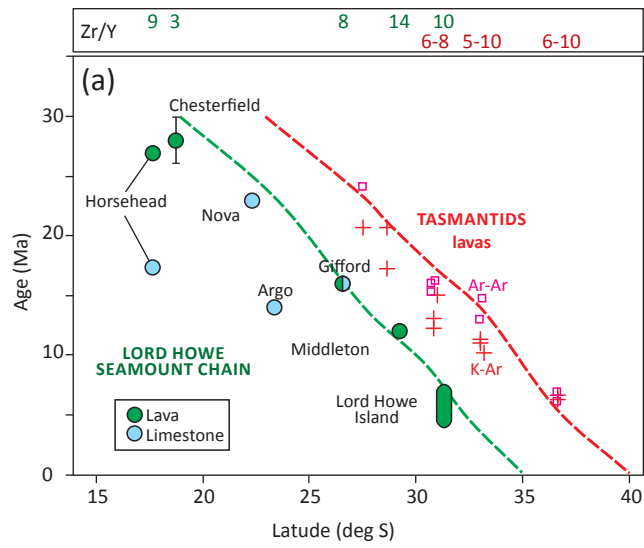
Location	Dredge	GNS #	147Sm/144Nd	143/144Nd meas	±2se	Age (Ma)	143Nd/144Nd init
Lord Howe Seamount Chain							
Horsehead	ECOSAT DR15Bi	P82218A	0.1609	0.512739	7	28	0.512711
Chesterfield	ECOSAT DR16Ai	P82221	0.1545	0.512826	7	27	0.512799
Lord Howe Island	na	GD6060	0.1303	0.512735	6	7	0.512729
Middleton Reef	NORFANZ DR49	P69722	0.1271	0.512883	8	12	0.512873
New Caledonia Basin margins							
Le Noroit	ECOSAT DR11Fi	P82196	0.1283	0.512917	6	64	0.512863
Lansdowne Bank	ECOSAT DR17Aiv	P82232	0.1672	0.512896	7	100	0.512787
Nereus Reef	ECOSAT DR18Bi	P82239	0.1574	0.512847	6	100	0.512744
Nereus Reef	ECOSAT DR18Bi	P82239 dup	0.1574	0.512837	8	100	0.512734
Nereus Reef	ECOSAT DR18Bii	P82240	0.1164	0.512951	9	100	0.512875
Nereus Reef	ECOSAT DR18Bii	P82240 dup	0.1164	0.512950	8	100	0.512874
Eocene-Oligocene backarc basin basalts							
Rennell Ridge SW side	GEORSTOM3 DR301A	P78604	0.2537	0.513012	8	38	0.512949
South Rennell Trough	GEORSTOM3 DR308A	P78613	0.2018	0.512996	8	28	0.512959
D'Entrecasteaux Ridge	GEORSTOM3 DR316-23	P78622	0.1669	0.513101	9	40	0.513057
Rennell Ridge NE side	ECOSAT DR03Ai	P82182	0.1503	0.512798	8	40	0.512759
West Torres Plateau	ECOSAT DR04Aii	P82188 rind	0.2006	0.512881	7	35	0.512835
West Torres Plateau	ECOSAT DR04Aii	P82188 inside	0.1973	0.512804	6	35	0.512759
East Laperouse Ridge	ECOSAT DR06A	P82193	0.1606	0.512727	8	35	0.512690
South Rennell Trough	ECOSAT DR14Ei	P82204	0.1916	0.51264	7	28	0.512605
South Rennell Trough	ECOSAT DR14Eiii	P82206	0.1539	0.512659	8	28	0.512631

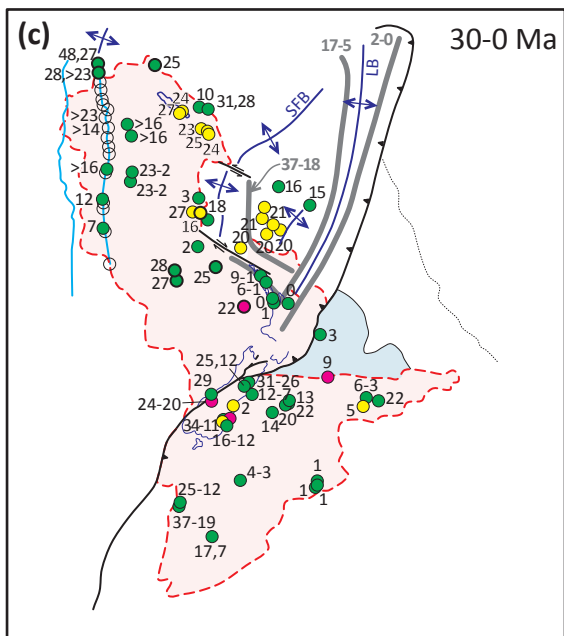
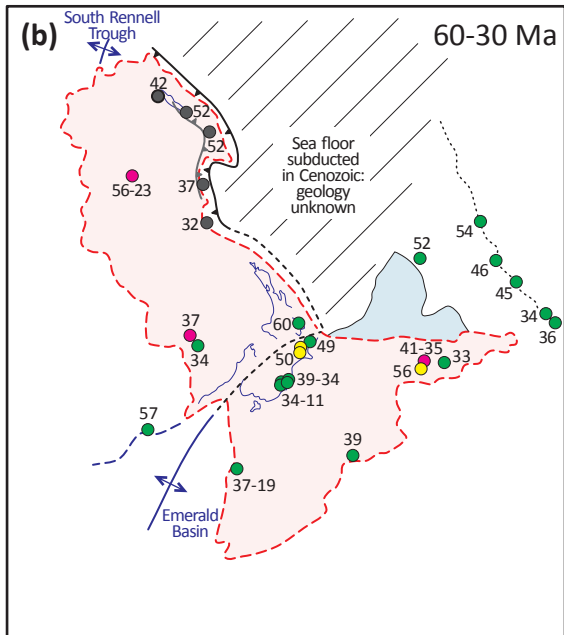
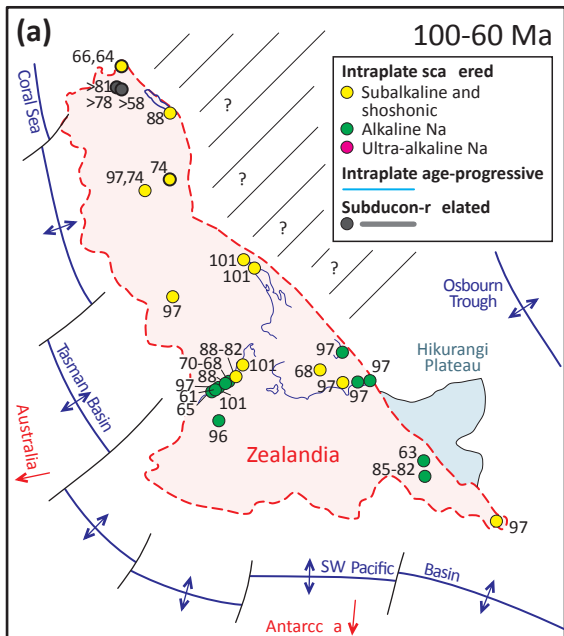




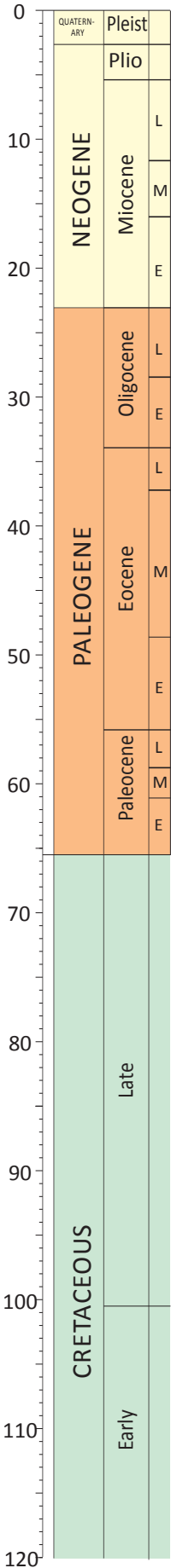




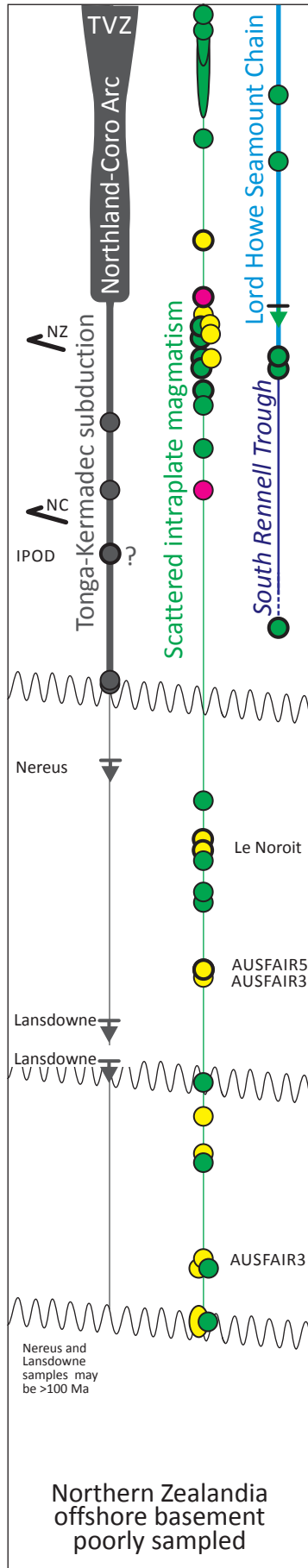




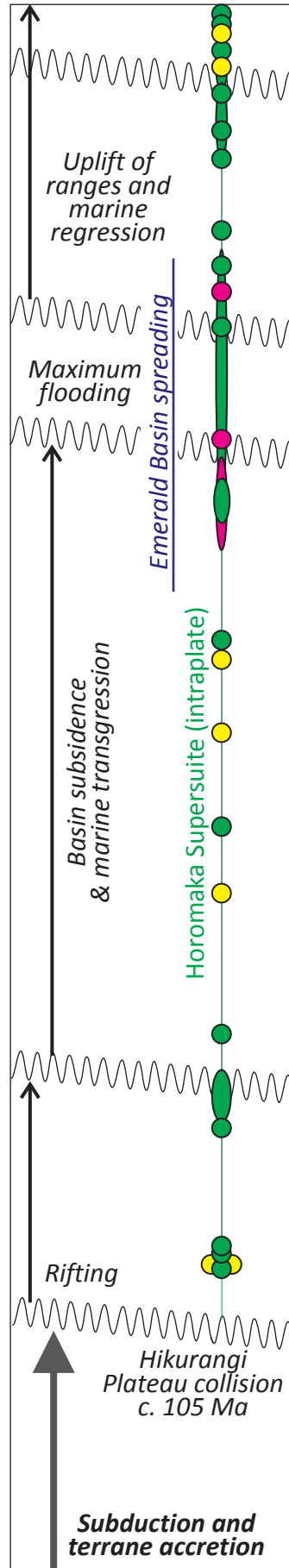
Age (Ma)



NORTHERN ZEALANDIA



SOUTHERN ZEALANDIA



Compositions

- Intraplate scattered
- Subalkaline and shoshonitic
- Alkaline Na
- Ultra-alkaline Na
- Intraplate age-progressive
- Subduction-related

Ages

- New
- Minimum, new
- Published

Ophiolitic allochthon obduction

New Caledonia and New Zealand